AN EXPERIMENTAL STUDY OF THE EFFECTIVENESS OF PLANT SCALE NATURAL GAS ABSORBERS

By

WILLIAM RUSS OWENS II

Bachelor of Science
University of Arkansas
Fayetteville, Arkansas
1966

Master of Science
Oklahoma State University
Stillwater, Oklahoma
1968

Submitted to the Faculty of the Graduate College
of the Oklahoma State University
in partial fulfillment of the requirements
for the Degree of
DOCTOR OF PHILOSOPHY
May, 1973

AN EXPERIMENTAL STUDY OF THE EFFECTIVENESS OF PLANT SCALE NATURAL GAS ABSORBERS

Thesis Approved:

R. N. Maddox
Thesis Adviser

John H. Erbar

James E. Shamblen

John B. West

D. D. Dunham
Dean of the Graduate College

ACKNOWLEDGMENT

I wish to thank Professor Robert N. Maddox for serving as my research adviser throughout my graduate program. His counsel and encouragement have been greatly appreciated. I am indebted to Oklahoma State University for financial support provided through an NDEA Title IV Fellowship.

With regards to this work, I am indebted to Cities Service Oil Company for making available their Ambrose Gasoline Plant in Blackwell, Oklahoma for this series of tests. I wish to thank Cities Service Oil Company and Phillips Petroleum Company of Bartlesville, Oklahoma for rendering chromatograph analyses of samples obtained. I also thank the Natural Gasoline Processors Association for help in coordinating the various company level activities required to obtain these tests.

Finally, I would like to thank my family for their constant encouragement during my graduate program.

TABLE OF CONTENTS

LIST OF TABLES

LIST OF FIGURES

CHAPTER I

INTRODUCTION

Test data for plant-scale natural gas absorbers have been obtained to determine their effectiveness. Overall absorber efficiencies have been taken to be about 30 to 50 per cent for design calculations, but no recent plant scale test information was available to substantiate these values.

Based upon two points an attempt was made to show that absorber efficiencies were higher than 30 to 50 per cent. The first point, developed during a study of tray-by-tray calculations, was that the terminal trays of an absorber experienced 80 per cent of the total absorption (16, 17). In this case, the contribution made by additional trays in the interior section of the absorber could be overshadowed by low efficiencies of the high mass transfer terminal trays. The second point resulted from improved methods of analyzing the samples and of predicting thermodynamic properties which were not available when the majority of absorber studies were being made.

Two identical parallel absorbers at the Cities Service Oil Company Ambrose Gasoline Plant were operated with common feeds and different numbers of trays. Gas samples for the rich and dry gases were analyzed on site, while rich and lean oil samples were analyzed at the Phillips Petroleum Company Research Laboratory.

Results from these tests were compared with rigorous tray-by-tray results with various numbers of ideal stages to determine the best

estimate of the number of ideal stages required to produce comparable results. A comparison of the parallel operating towers was presented to directly show the effect of the actual number of stages.

CHAPTER II

BACKGROUND

Hydrocarbon absorbers constitute a particular class of countercurrent mass transfer equipment. An oil stream is introduced at the top of a contacting device and flows down past a rising gas stream. In the process, varying amounts of heavier components that make up the gas are absorbed by the oil (See Figure 1.). The methods for handling absorber calculations are developed in the following sections.

For a single component, a material balance can be written for one stage as: the sum of the vapor and liquid leaving the ith stage is equal to the sum of the liquid entering the stage from the stage above and the vapor rising from the stage below.

$$v_i + \ell_i = v_{i+1} + \ell_{i-1} \tag{1}$$

Lower case ℓ denotes the liquid molar rate of the jth component and v, the vapor molar rate of component j. The subscript i indicates the equilibrium stage numbered from the top of the tower down. Thus v_{i+1} is the molar liquid rate of component j leaving the i+1 stage. To avoid using double subscripts in presenting the absorber mathematics, all equations are developed for the jth component and the j is omitted.

A convenient relationship between the liquid and vapor of component j in equilibrium on the ith stage is the absorption factor, A.

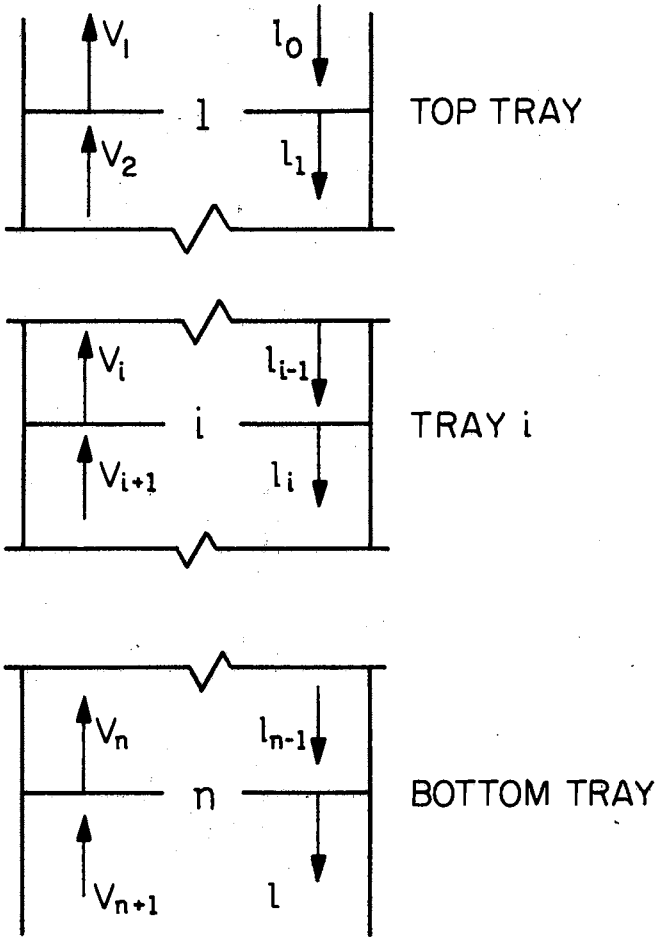

Figure 1. A Simple Absorber

$$A_i \equiv \frac{L_i}{V_i K} = \frac{\ell_i}{v_i} \tag{2}$$

In this equation L_i is the total molar rate of the liquid leaving the ith stage; V_i, the molar vapor rate; and K the equilibrium constant for the jth component. The absorption factor is convenient for two reasons. First it allows the material balance equation to be developed in terms of the component vapor rates or the liquid rates. Second, the absorption factors for each component can be expressed in terms of the total molar rates and the individual component equilibrium constant. This allows the material balance for an absorber with n trays to be expressed as a single equation in terms of the known rates--the lean oil, ℓ_o, and the rich gas, v_{n+1}--and the absorption factor on each stage.

Beginning with the top tray, the vapor entering this stage can be obtained by rearranging equation 1.

$$v_2 = \ell_1 + v_1 - \ell_o$$

Using the absorption factor on the top tray the equation becomes

$$v_2 = v_1(A_1 + 1) - \ell_o$$

Using the absorption factor of the second stage, the liquid leaving stage 2 is

$$\ell_2 = A_2 v_2 = v_1(A_1 A_2 + A_2) - \ell_o A_2 \tag{3}$$

By repeated application of the material balance equation and the absorption factor definition, an equation is developed for the rich oil, ℓ_n, as a function of the component dry gas and lean oil rates, v_{n+1} and ℓ_o, and the individual tray absorption factors.

$$\ell_n = V_{n+1}(A_1A_2A_3 \ldots A_n + A_2A_3 \ldots A_n + \ldots + A_n) - \ell_o (A_2 \ldots A_n + \ldots + A_n) \quad (4)$$

Applying the criterion of an overall component material balance to this equation and rearranging yields equation 5

$$v_1 = v_{n+1}\left[\frac{1}{\Sigma_A + 1}\right] + \ell_o\left[1 - \frac{\Pi_A}{\Sigma_A + 1}\right] \quad (5)$$

where

$$\Sigma_A = A_1A_2 \circ \ldots \circ A_n + A_2 \ldots \circ A_n + \ldots + A_n$$

$$\Pi_A = A_1A_2 \ldots \circ A_n .$$

Using this equation, the dry gas rate for each component can be calculated knowing the feed rates for the component, the L/V ratio on each stage, and the equilibrium constant for the component at the conditions of the individual stage.

The equations developed above represent the fundamentals required for calculating component distribution for an absorber operating with specified feed rates and column operating conditions.

The solutions to the rigorous material balance and heat balance equations were obtained by a computer program written by Spear (21) employing the Sujata technique (22). Thermodynamic data for the components were obtained from least-square fitted equilibrium and enthalpy values from the Engineering Data Book (5) and from the Chao-Seader correlation (2). In addition to these two sources, the Chao-Seader correlation was incorporated with the tray-by-tray program to give results that reflect the dependence of the K-values on the individual tray compositions.

Fundamentally, the Sujata procedure solves the set of simultaneous linear equations describing the component material balance on each tray to determine the composition profile. These component rates are used to generate the heat balance calculations about each stage. Errors in the heat balances are used to predict new temperatures for each stage. With a new temperature profile, new material balances are calculated and the procedure iterates until changes in successive temperature profiles are within specified limits.

For this calculational method the equilibrium stage material balance has been generalized to include a feed stream in addition to the counter-current vapor-liquid streams that enter and leave the ith stage. The sketch for this balance is shown in Figure 2. For any component, j, the material balance of equation 1 has been ammended to include a separate feed to that stage.

$$[-\ell_{i-1} + \ell_i + v_i - v_{i+1} = f_i]_{\text{component } j} \tag{6}$$

Then using the equilibrium relationship defining the stripping factor as the reciprocal of the absorption factor,

$$v_i = K\frac{V_1}{L_1}\ell_i = S_i\ell_i \tag{7}$$

the general equation can be written as follows.

$$-\ell_{i-1} + (1 + S_i)\ell_i - S_{i+1}\ell_{i+1} = f_i \tag{8}$$

For an n tray absorber, the n material balance equations are linearly independent in terms of the ℓ's and can be expressed in matrix notation. Spear's program (27) utilizes matrix algebra to obtain the solution to these equations.

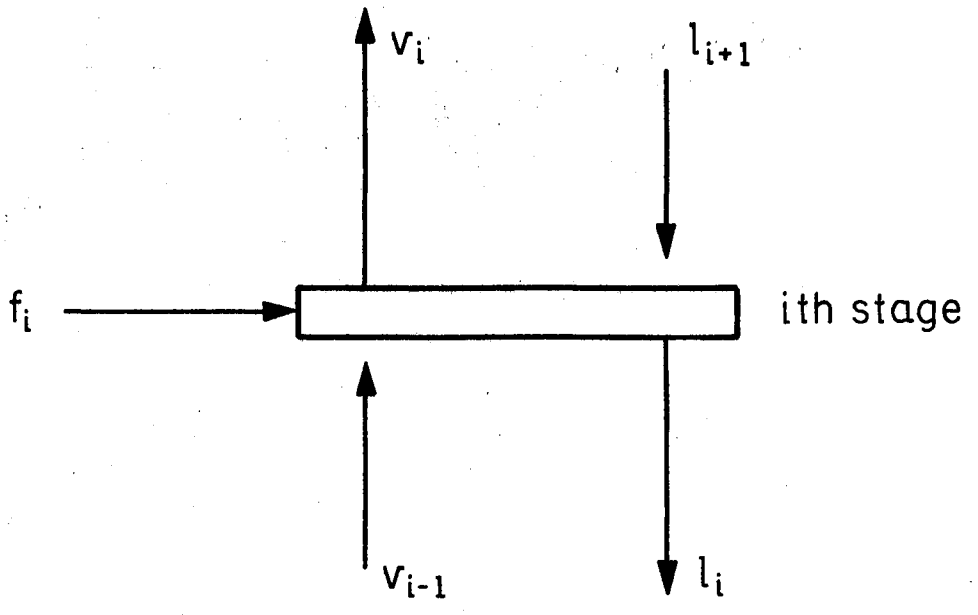

where f = moles of particular component entering as feed on the tray;

v = moles of particular component vapor

l = moles of particular component liquid.

Figure 2. A Complex Ideal Tray

To evaluate the stripping factor for each component on each tray some estimate of the L/V ratio and the equilibrium constant are required. In the procedure presented by Spear, the equilibrium constant is a function of temperature only. This reduces the requirements for evaluating the stripping factor, the L/V profile and the temperature profile. Initial L/V and temperature profiles required are revised by subsequent calculations. The new total liquid rate on any tray is the sum of the calculated individual component rates and the new total vapor rates are found by overall material balance.

Once the correct rates have been found for a specified temperature profile, this profile must be checked for validity. This is done by writing a heat balance around each stage such that

$$G_i \approx \{\text{feed enthalpy}\} - \{\text{product enthalpy}\} - \{\text{heat losses}\} \quad (9)$$

With this definition, G_i equals zero for the correct temperature profiles. By considering G_i a total differential quantity dG_i, it can be expressed as a function of the temperatures of the tray and its nearest neighbors

$$dG_i = \frac{\partial G_i}{\partial t_{i-1}} dt_{i-1} + \frac{\partial G_i}{\partial t_i} dt_i + \frac{\partial G_i}{\partial t_{i+1}} dt_{i+1} \quad (10)$$

From this relationship, a set of n equations is formed. The linearly independent variable is dt_i, the change in temperature on each stage required to satisfy the heat balance equations. The coefficient matrix is formed of the total heat capacity of the streams entering and leaving the stage. The new temperatures are calculated by equation 11.

$$t_{i,new} = t_{i,old} + dt_i \quad (11)$$

With the new L/V and temperature profile the procedure begins again. This looping continues until successive temperatures and liquid flow rates are within specified limits. When they are, solution has been found for the specified conditions.

Thermodynamic Properties

Although this thesis does not represent an effort to evaluate thermodynamic properties of the components involved, it necessarily reflects such values used in the theoretical calculations. For example, for a given basis of thermodynamic information and a specified absorber operating condition, a product distribution and temperatures can be calculated. However, slight differences in the equilibrium values at a given temperature would lead to different product compositions. This would change the heat balance which would produce different product temperatures producing further variation in the equilibrium values. By the same reasoning a minor change in the enthalpies would produce different product temperatures, changing the equilibrium values and thus the product rates.

These small variations in the calculated solution have a large impact when dealing with towers with four or more theoretical trays and components with absorption factors less than one. For components with absorption factors of this magnitude the additional stages yield small increases in component recovery. These components are, however, the ones of interest in evaluating the efficiency of the absorber.

Thermodynamic properties used in this work were obtained from the NGPA K and H Value Computer Program (14). Equilibrium values are predicted by the Chao-Seader (2) correlation and enthalpy values by a

procedure of Erbar (8). These values were employed either directly by combination of computer programs or indirectly by polynomial fit of predicted values.

The 1957 NGPSA Engineering Data Book (5) supplied an additional source of thermodynamic properties. These values served two purposes. First, they provided an order of magnitude check of the values predicted by the Chao-Seader scheme. Second, they point out the changes in an absorber solution brought about by slight differences in thermodynamic data.

Coefficients from the least-squares fit of the equilibrium and enthalpy values predicted by the NGPA K and H Value Computer Program are presented in Appendix C for the base case of each absorber test period. The coefficients from the alternate source are presented for the base case of the A24 test period.

CHAPTER III

DESCRIPTION OF EQUIPMENT

Absorber test data were obtained from the facilities of the Cities Service Oil Company Ambrose Gasoline Plant. This plant is located in Blackwell, Oklahoma, and nominally handles 270 million standard cubic feet of natural gas per day. This flow is directed through two parallel absorbers as shown in Figure 3. Each of the eight foot in diameter absorbers has 24 trays and two intercoolers. For these tests the intercoolers were not employed.

Process

The inlet gas is combined with recompressor gas as it enters the plant. Glycol is injected to prevent hydrate formation during cooling. The gas is cooled first in the gas-gas exchanger and then further cooled in the gas chiller. The glycol and water are removed and the stream is split for feeding the absorbers. The product gas, or dry gas, from the absorbers is metered, combined, and scrubbed again before leaving the plant site.

The lean oil is the bottom product from a low pressure still and is cooled on the shell side of the oil-oil exchanger with the rich oil being on the tube side. The lean oil is split and metered before being introduced into the absorbers. The combined rich oil from both

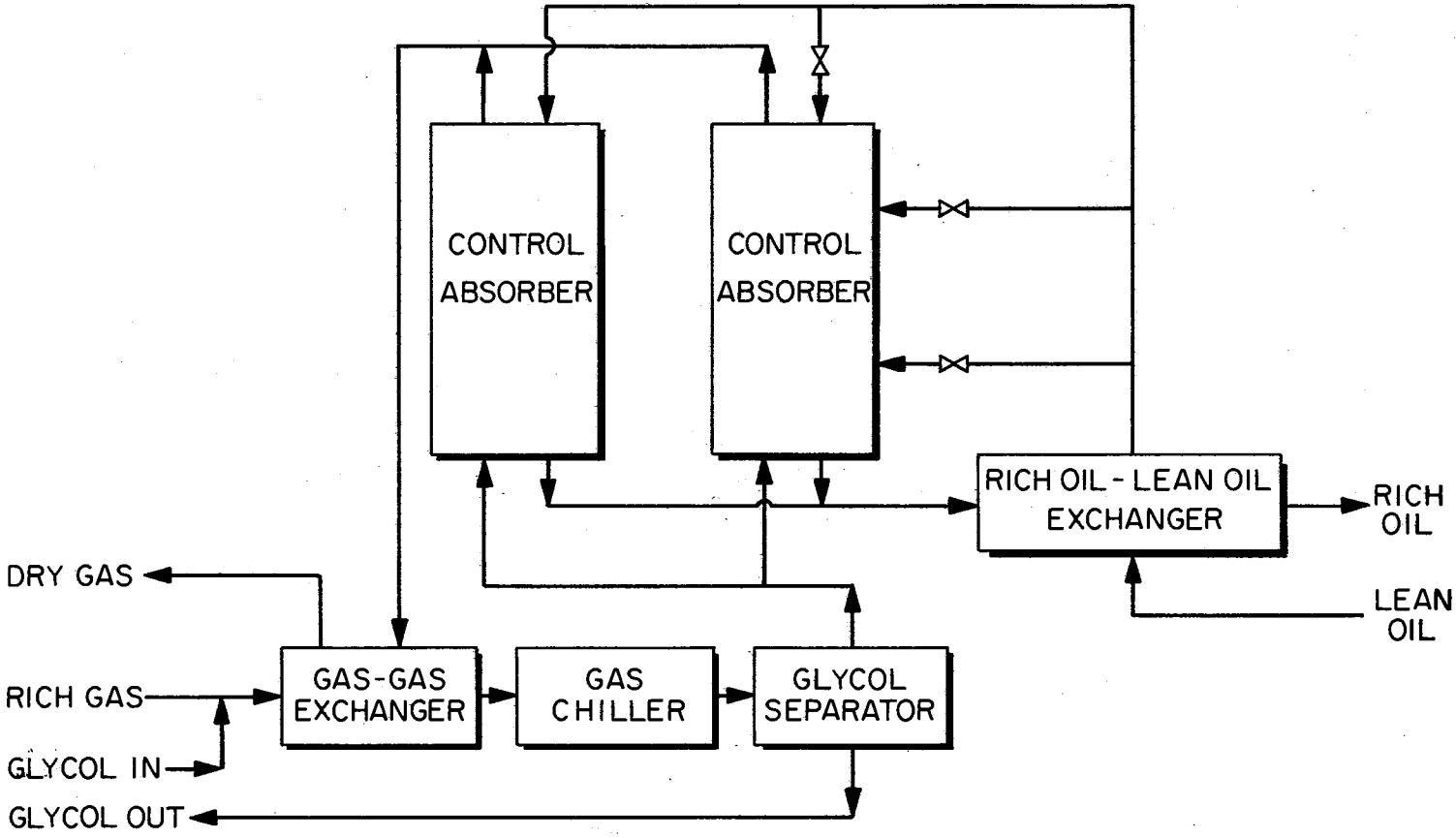

Figure 3. Schematic Diagram of Ambrose Gasoline Plant Absorber Section

absorbers is used to cool the lean oil and then passed on to the stills to remove the recovered light hydrocarbons.

Absorbers

The parallel absorbers are 57 feet tall and eight feet in diameter. Each contains 24 split-flow sieve trays on 24 inch center spacing. The trays are perforated with 5/32 inch holes on 3/8 inch triangular pitch and are equipped with two inch wiers on both the inlet and outlet of the tray.

Each column has two liquid intercoolers, one on the eighth tray and the other on the sixteenth tray. Each intercooler has a 2 MM Btu/hr capacity. Design capacities for the absorbers are

- 142 MM scf/day Rich Gas
- 530 gpm Lean Oil
- 753 psig Maximum Working Pressure.

Modifications

For the duration of these runs one of the absorbers was maintained as the base case--a simple absorber with 24 trays. This absorber was considered the Control Absorber.

The second absorber was modified to allow the lean oil to be introduced on either the eighth or sixteenth tray through the return line from the intercooler. This absorber served as the Test Absorber.

Instrumentation

Three types of instruments were used to monitor the operation of the absorbers. They were temperature indicators, pressure indicators, and flow recorders. Specific characteristics of each class follow.

Temperature indicators available were glass thermometers in commercial thermowells. Range of the thermometers was 0-120°F with 2° increments.

Several thermowells were not equipped with working thermometers. These were associated with the column intercoolers and were not required for operation. They could have provided additional data, as they would have indicated the approximate temperature profile of the absorber.

Pressure measurements were made at the rich oil exit port of each column. Bourdon pressure gages with 0-1000 psig ranges and 10 psi increments were used.

The lean oil and the dry gas rates for each absorber were obtained from orifice meters. For the gas rates, 9.5 inch ID orifices were used in 14 inch pipe. The lean oil rate to each absorber was measured using a 4.25 inch orifice in the 6.025 inch line. An example of the calculation used to convert the orifice readings to flow rates is presented in Appendix D.

CHAPTER IV

PROCEDURES

Simultaneous tests were conducted on two parallel natural gas absorbers to determine their comparative effectiveness. These absorbers were operated at identical conditions but with a different number of trays. The tests were run at the Cities Service Ambrose Gasoline Plant in Blackwell, Oklahoma, on Monday, November 4, 1968. At 4:00 p.m., Sunday, November 3, the intercoolers were shut down on both absorbers. The lean oil feed to the first absorber was introduced in the lower intercooler return port on the eighth tray. The second absorber operated as a simple 24 tray absorber. When tests were completed on this configuration, the lean oil feed of the first absorber was raised to the sixteenth tray, the upper intercooler return.

The absorbers were allowed 18 hours to reach steady state operation before the first test period, four hours for the second. The criteria used to define steady state operation were constant dry gas rates and product temperatures. The difference in the times allowed for the system to reach steady state was a matter of available time. However, the above criteria were met in both cases.

A simple absorber with n trays and C components can be uniquely defined by specifying

$$2C + 2n + 5$$

variables (15). To adequately define these, values for the following variables were obtained.

pressure--assumed constant in each stage		n
heat leak in each stage--assumed zero in each stage		n
lean oil composition	C	
lean oil rate and temperature		2
rich gas composition	C	
rich gas temperature		1
dry gas rate		1
number of stages		1
		2C + 2n + 5

Specific temperatures for the absorbers were taken on the common feed, the combined dry gas stream, and the individual rich oil streams. The rich gas temperature was measured at the exit from the gas chillers. The lean oil temperature was taken at the exit of the lean oil-rich oil exchanger. A combined stream dry gas temperature was obtained at the inlet to the gas-gas exchanger. This was the only available place to measure the dry gas temperature. Rich oil temperatures were measured at the outlet ports of the individual absorber.

Tower pressure was measured at the rich oil exit port of the absorber. Top tower pressure was taken from the dry gas flow recorder for each unit.

Since the feed streams were common to both absorbers, only one sample was required for each set of parallel tests. The lean oil sample was taken at the lean oil charge pump. The rich gas sample was taken at the exit from the gas chiller. Product streams were sampled individually. The rich oil sample was taken from connections on the bottom of the level gage of each tower. The dry gas sample was drawn from connections for the flow meter for each tower.

All temperature, pressure, and flow points were monitored to indicate steady state operation. When steady state operation was indicated, a complete complement of temperatures and pressures was recorded, a procedure requiring twenty minutes. After that, all samples were caught and the temperature and pressure measurements were repeated.

Sample bombs for the vapor and liquid samples were provided by Cities Service Oil Company. They were 303 stainless steel, 2000 pound test, MGM bombs fitted with two Hoke valves. The gas samples were obtained by purging the stream through the bomb, closing the exit valve, and then the entrance valve. Liquid samples were obtained by first purging the sample line up to the bomb. A 60 ml sample was then obtained by water displacement.

Gas samples were analyzed on site and components reported were: carbon dioxide, nitrogen, methane through normal pentane, and C_6 fraction. Liquid samples were analyzed by Phillips Petroleum Company Research Laboratory at Bartlesville, Oklahoma, in cooperation with this test program. An outline of their procedure and results from all analyses can be found in Appendix A.

CHAPTER V

PRESENTATION OF RESULTS

Results from the plant scale absorber tests are presented in Tables I to IX. Four test periods were made, two at a time on the parallel absorbers. In each set one absorber was maintained as the control case with the full compliment of trays and the second was the test case. A description of each test period follows:

A24	Control	This absorber was operated with the full 24 trays.
A8	Test	This absorber was operated at identical conditions to the control case except only 8 trays were employed.
B24	Control	Operating conditions for this test period are similar to those of the A24 test period with slight changes due to changes in the overall plant operation.
B16	Test	Sixteen trays were employed in this absorber.

The results for these test periods are presented in the following tables. For each test period two tables present the reported compositions and flow rates for the feed and product streams in addition to the material balance compositions.

For convenience, each case is based upon 100 moles of rich gas per hour.

TABLE I

EXPERIMENTAL DATA FOR A24 TEST PERIOD

Trays = 24	Pressure = 545 psia			
Component	Composition, Mole Per Cent			
	Lean Oil	Rich Gas	Rich Oil	Dry Gas
Carbon Dioxide	0.0	0.235	0.10	0.231
Nitrogen	0.0	5.265	0.52	5.649
Methane	0.0	82.053	19.40	86.150
Ethane	0.04	7.183	9.50	6.417
Propane	0.03	3.518	15.10	1.553
I-Butane	0.0	0.388	2.55	0.0
N-Butane	0.10	0.890	5.60	0.0
I-Pentane	0.25	0.189	1.04	0.0
N-Pentane	0.49	0.199	1.10	0.0
2-Methylpentane	0.28	0.0	0.22	0.0
3-Methylpentane	0.16	0.0	0.10	0.0
N-Hexane	0.58	0.04	0.31	0.0
Cyclohexane	0.87	0.0	0.38	0.0
N-Heptane	4.90	0.04	2.17	0.0
N-Octane	10.50	0.0	4.80	0.0
N-Nonane	10.50	0.0	4.70	0.0
N-Decane	16.70	0.0	7.50	0.0
N-Undecane	26.90	0.0	12.20	0.0
N-Dodecane	20.90	0.0	9.50	0.0
N-Tridecane	6.80	0.0	3.21	0.0
Rates	493.0 gpm	*	*	6.708 MM scf/hr
Temperatures, °F	32	9	22	45

*No facilities available to measure this quantity.

TABLE II

MATERIAL BALANCE FOR A24 TEST PERIOD

Basis: 100 mole/hr Rich Gas

Component	Moles			
	Lean Oil	Rich Gas	Rich Oil	Dry Gas
Carbon Dioxide	0.0	0.235	0.022	0.213
Nitrogen	0.0	5.265	0.050	5.215
Methane	0.0	82.053	2.516	79.537
Ethane	0.003	7.183	1.262	5.924
Propane	0.002	3.518	2.086	1.434
I-Butane	0.0	0.388	0.388	0.0
N-Butane	0.006	0.890	0.896	0.0
I-Pentane	0.016	0.189	0.205	0.0
N-Pentane	0.031	0.199	0.230	0.0
2-Methylpentane	0.019	0.0	0.019	0.0
3-Methylpentane	0.010	0.0	0.010	0.0
N-Hexane	0.037	0.040	0.077	0.0
Cyclohexane	0.056	0.0	0.056	0.0
N-Heptane	0.313	0.040	0.353	0.0
N-Octane	0.670	0.0	0.670	0.0
N-Nonane	0.670	0.0	0.670	0.0
N-Decane	1.066	0.0	1.066	0.0
N-Undecane	1.718	0.0	1.718	0.0
N-Dodecane	1.334	0.0	1.334	0.0
N-Tridecane	0.434	0.0	0.434	0.0
Rates, Moles	6.385	100.00	14.062	92.323

$$\text{Feed Ratio} = \frac{\text{lean oil rate}}{\text{rich gas rate}} = 0.06385$$

TABLE III

EXPERIMENTAL DATA FOR A8 TEST PERIOD

Trays = 8	Pressure = 536 psia			
Component	Composition, Mole Per Cent			
	Lean Oil	Rich Gas	Rich Oil	Dry Gas
Carbon Dioxide	0.0	0.235	0.12	0.238
Nitrogen	0.0	5.265	0.55	5.792
Methane	0.0	82.053	22.90	86.290
Ethane	0.04	7.183	9.80	6.273
Propane	0.03	3.518	14.20	1.372
I-Butane	0.0	0.388	2.14	0.018
N-Butane	0.10	0.890	4.60	0.017
I-Pentane	0.25	0.189	0.80	0.0
N-Pentane	0.49	0.199	0.88	0.0
2-Methylpentane	0.28	0.0	0.20	0.0
3-Methylpentane	0.16	0.0	0.10	0.0
N-Hexane	0.58	0.040	0.29	0.0
Cyclohexane	0.87	0.0	0.43	0.0
N-Heptane	4.90	0.040	2.08	0.0
N-Octane	10.50	0.0	4.50	0.0
N-Nonane	10.50	0.0	4.60	0.0
N-Decane	16.70	0.0	7.30	0.0
N-Undecane	26.90	0.0	12.00	0.0
N-Dodecane	20.90	0.0	9.40	0.0
N-Tridecane	6.80	0.0	3.11	0.0
Rates	509.0 gpm	*	*	6.903 MM scf/hr
Temperatures, °F	32	9	22	45

*No facilities available to measure this quantity.

TABLE IV

MATERIAL BALANCE FOR A8 TEST PERIOD

Basis: 100 mole/hr Rich Gas

Component	Moles			
	Lean Oil	Rich Gas	Rich Oil	Dry Gas
Carbon Dioxide	0.0	0.235	0.016	0.219
Nitrogen	0.0	5.265	0.0	5.265
Methane	0.0	82.053	2.617	79.436
Ethane	0.003	7.183	1.416	5.770
Propane	0.002	3.518	2.258	1.262
I-Butane	0.0	0.388	0.371	0.017
N-Butane	0.006	0.890	0.880	0.016
I-Pentane	0.016	0.189	0.205	0.0
N-Pentane	0.031	0.199	0.230	0.0
2-Methylpentane	0.018	0.0	0.018	0.0
3-Methylpentane	0.010	0.0	0.010	0.0
N-Hexane	0.037	0.040	0.077	0.0
Cyclohexane	0.056	0.0	0.056	0.0
N-Heptane	0.313	0.040	0.353	0.0
N-Octane	0.670	0.0	0.670	0.0
N-Nonane	0.670	0.0	0.670	0.0
N-Decane	1.065	0.0	1.065	0.0
N-Undecane	1.716	0.0	1.716	0.0
N-Dodecane	1.333	0.0	1.333	0.0
N-Tridecane	0.434	0.0	0.434	0.0
Rates, moles	6.380	100.00	14.395	91.985

Feed Ratio = $\frac{\text{lean oil rate}}{\text{rich gas rate}}$ = 0.0638

TABLE V

EXPERIMENTAL DATA FOR B24 TEST PERIOD

Trays = 24	Pressure = 575 psia			
Component	Composition, Mole Per Cent			
	Lean Oil	Rich Gas	Rich Oil	Dry Gas
Carbon Dioxide	0.0	0.2180	0.16	0.251
Nitrogen	0.0	5.353	0.45	5.364
Methane	0.0	81.624	25.60	86.434
Ethane	0.04	7.331	10.90	6.380
Propane	0.03	3.676	16.00	1.524
I-Butane	0.0	0.410	2.73	0.024
N-Butane	0.07	0.913	6.50	0.023
I-Pentane	0.22	0.178	1.38	0.0
N-Pentane	0.46	0.176	1.57	0.0
2-Methylpentane	0.38	0.0	0.57	0.0
3-Methylpentane	0.15	0.0	0.17	0.0
N-Hexane	0.56	0.070	0.25	0.0
Cyclohexane	0.79	0.0	0.09	0.0
N-Heptane	4.50	0.051	1.20	0.0
N-Octane	10.30	0.0	3.20	0.0
N-Nonane	10.40	0.0	3.60	0.0
N-Decane	16.70	0.0	5.80	0.0
N-Undecane	27.10	0.0	9.50	0.0
N-Dodecane	21.20	0.0	7.40	0.0
N-Tridecane	7.20	0.0	2.93	0.0
Rates	502.0 gpm	*	*	6.998 MM scf/hr
Temperature, °F	34	11	24	47

*No facilities available to measure this quantity.

TABLE VI

MATERIAL BALANCE FOR B24 TEST PERIOD

Basis: 100 mole/hr Rich Gas

Component	Moles			
	Lean Oil	Rich Gas	Rich Oil	Dry Gas
Carbon Dioxide	0.0	0.218	0.0	0.218
Nitrogen	0.0	5.353	0.583	4.770
Methane	0.0	81.624	4.844	76.780
Ethane	0.002	7.331	1.666	5.667
Propane	0.002	3.676	2.324	1.354
I-Butane	0.0	0.410	0.389	0.021
N-Butane	0.004	0.913	0.897	0.020
I-Pentane	0.013	0.178	0.191	0.0
N-Pentane	0.028	0.176	0.204	0.0
2-Methylpentane	0.017	0.0	0.017	0.0
3-Methylpentane	0.009	0.0	0.009	0.0
N-Hexane	0.034	0.070	0.104	0.0
Cyclohexane	0.047	0.0	0.047	0.0
N-Heptane	0.270	0.051	0.321	0.0
N-Octane	0.617	0.0	0.617	0.0
N-Nonane	0.623	0.0	0.623	0.0
N-Decane	1.000	0.0	1.000	0.0
N-Undecane	1.623	0.0	1.623	0.0
N-Dodecane	1.270	0.0	1.270	0.0
N-Tridecane	0.431	0.0	0.431	0.0
Rates, Moles	5.990	100.00	17.160	88.830

$$\text{Feed Ratio} = \frac{\text{lean oil rate}}{\text{rich gas rate}} = 0.0599$$

TABLE VII

EXPERIMENTAL DATA FOR B16 TEST PERIOD

Trays = 16	Pressure = 656 psia			
Component	Composition, Mole Per Cent			
	Lean Oil	Rich Gas	Rich Oil	Dry Gas
Carbon Dioxide	0.0	0.218	0.16	0.248
Nitrogen	0.0	5.353	0.0	5.471
Methane	0.0	81.624	31.70	86.652
Ethane	0.04	7.331	10.90	6.230
Propane	0.03	3.676	13.30	1.399
I-Butane	0.0	0.410	1.99	0.0
N-Butane	0.07	0.913	4.10	0.0
I-Pentane	0.22	0.178	0.48	0.0
N-Pentane	0.46	0.176	0.56	0.0
2-Methylpentane	0.28	0.0	0.15	0.0
3-Methylpentane	0.15	0.0	0.07	0.0
N-Hexane	0.56	0.070	0.21	0.0
Cyclohexane	0.79	0.0	0.27	0.0
N-Heptane	4.50	0.051	1.62	0.0
N-Octane	10.30	0.0	3.80	0.0
N-Nonane	10.40	0.0	3.90	0.0
N-Decane	16.70	0.0	6.20	0.0
N-Undecane	27.10	0.0	10.10	0.0
N-Dodecane	21.20	0.0	7.80	0.0
N-Tridecane	7.20	0.0	2.69	0.0
Rates	502.0 gpm	*	*	7.160 MM scf/hr
Temperatures, °F	34	11	23	47

*No facilities available to measure this quantity.

TABLE VIII

MATERIAL BALANCE FOR B16 TEST PERIOD

Basis: 100 mole/hr Rich Gas

Component	Moles			
	Lean Oil	Rich Gas	Rich Oil	Dry Gas
Carbon Dioxide	0.0	0.218	0.0	0.218
Nitrogen	0.0	5.353	0.426	4.927
Methane	0.0	81.624	3.656	77.968
Ethane	0.002	7.331	1.726	5.606
Propane	0.002	3.676	2.419	1.259
I-Butane	0.0	0.410	0.410	0.0
N-Butane	0.004	0.913	0.917	0.0
I-Pentane	0.013	0.178	0.191	0.0
N-Pentane	0.027	0.176	0.203	0.0
2-Methylpentane	0.017	0.0	0.017	0.0
3-Methylpentane	0.009	0.0	0.009	0.0
N-Hexane	0.033	0.070	0.103	0.0
Cyclohexane	0.047	0.0	0.047	0.0
N-Heptane	0.266	0.051	0.317	0.0
N-Octane	0.610	0.0	0.610	0.0
N-Nonane	0.615	0.0	0.615	0.0
N-Decane	0.988	0.0	0.988	0.0
N-Undecane	1.604	0.0	1.604	0.0
N-Dodecane	1.255	0.0	1.255	0.0
N-Tridecane	0.426	0.0	0.426	0.0
Rates, Moles	5.918	100.00	15.940	89.978

$$\text{Feed Ratio} = \frac{\text{lean oil rate}}{\text{rich gas rate}} = 0.05918$$

TABLE IX

SUMMARY OF ABSORBER CONDITIONS

Trays	A24	A8	B24	B16
Trays	24	8	24	16
Pressure, psia	545	536	575	565
Rates,* Moles				
lean oil	6.385	6.380	5.990	5.918
rich oil	14.062	14.395	17.160	15.940
dry gas	92.323	91.985	88.830	89.978
gas shrinkage	7.677	8.015	11.170	10.022
Temperatures, ^{o}F				
rich gas	9	9	11	11
lean oil	32	32	34	34
rich oil	22	22	24	23
dry gas	45	45	47	47
Recovery**				
methane	0.0307	0.0326	0.0593	0.0448
ethane	0.1752	0.1967	0.2269	0.2354
propane	0.5917	0.6413	0.6317	0.6567

*Basis: 100 mole/hr rich gas.

**Fraction of the component in the rich gas feed recovered in the rich oil.

A summary of the operating conditions and the light hydrocarbon recoveries are presented for each test period in Table IX.

CHAPTER VI

DISCUSSION OF RESULTS

The original data for each of the four test periods on plant scale absorbers were examined by material balance, phase, and heat balance calculations. Once the evaluation of the test data was completed, a direct comparison of each absorber was made with tray by tray solutions. Initially the number of ideal stages was varied to determine the effectiveness of the individual towers. Subsequently variations of pressure, oil characterization, and source of equilibrium values were studied to more accurately model each of the tests. The effect of experimental error was then investigated using an empirical model. Finally, the results from the parallel operating units were compared to each other.

Evaluation of Plant Test Data

To evaluate plant scale data, an organized program was developed to reduce the effect of errors that occurred in measuring process variables and stream compositions. The first step of this program was to complete the material balance for each test period.

During the plant tests samples of both feeds and both products were taken. Analyses of these samples were presented in Tables I, III, V, and VII.

Only the dry gas and lean oil rates were measured for each unit. The rich gas and rich oil rates were not measured due to a lack of facilities on the individual units. In order to complete the material balance from available information these rates must be calculated from measured quantities. The following scheme was used to complete the material balance for these test periods.

A specified fraction of the heavy components entering in the lean oil stream was assumed to leave the tower only in the rich oil stream. From the material balance calculations for the heavy fraction, the rich oil rate was expressed in the following relationship.

$$RO = LO \left[\frac{\bar{X}_{LO,\ Heavy\ Fraction}}{\bar{X}_{RO,\ Heavy\ Fraction}} \right] \qquad (12)$$

In this equation RO and LO are the rich oil and the lean oil rates while $\bar{X}_{RO,\ Heavy\ Fraction}$ and $\bar{X}_{LO,\ Heavy\ Fraction}$ are the concentrations for the components included in the heavy fraction of the respective streams. For each test period octane and heavier components were used as the heavy fraction basis.

Once the rich oil rate had been determined, the rich gas rate was calculated from overall material balance around the absorber. As a check, the rich oil composition was calculated from individual component material balances and compared with analytical results. Tables X, XI, XII, and XIII show these results. In each case the deviation between the two values has been expressed as the difference in moles from component material balance results. All flow rates have been based upon 100 moles of rich gas per hour to the unit. The sum of the deviations for the octane and heavier components must be zero as

TABLE X

COMPARISON OF RICH OIL COMPOSITIONS OBSERVED AND CALCULATED FOR A24 TEST PERIOD

Component	Composition, Mole Per Cent		
	Observed	Calculated	Deviation, Moles
Carbon Dioxide	0.10	0.155	-0.008
Nitrogen	0.52	0.353	0.023
Methane	19.40	17.895	0.213
Ethane	9.50	8.969	0.074
Propane	15.10	14.835	0.037
I-Butane	2.55	2.759	-0.030
N-Butane	5.60	6.375	-0.108
I-Pentane	1.04	1.458	-0.059
N-Pentane	1.10	1.638	-0.075
2-Methylpentane	0.22	0.127	0.013
3-Methylpentane	0.10	0.073	0.004
N-Hexane	0.31	0.548	-0.034
Cyclohexane	0.38	0.395	-0.002
N-Heptane	2.17	2.509	-0.048
N-Octane	4.80	4.768	0.005
N-Nonane	4.70	4.768	-0.010
N-Decane	7.50	7.583	-0.012
N-Undecane	12.20	12.214	-0.002
N-Dodecane	9.50	9.490	0.002
N-Tridecane	3.21	3.088	0.017
	100.0	100.00	0.00

TABLE XI

COMPARISON OF RICH OIL COMPOSITIONS OBSERVED AND CALCULATED FOR A8 TEST PERIOD

Component	Composition, Mole Per Cent		
	Observed	Calculated	Deviation, Moles
Carbon Dioxide	0.12	0.112	0.001
Nitrogen	0.55	-0.436	0.142
Methane	22.90	18.610	0.617
Ethane	9.80	9.832	-0.004
Propane	14.20	15.685	-0.214
I-Butane	2.14	2.580	-0.063
N-Butane	4.60	6.118	-0.218
I-Pentane	0.80	1.424	-0.090
N-Pentane	0.88	1.600	-0.104
2-Methylpentane	0.20	0.124	0.011
3-Methylpentane	0.10	0.071	0.004
N-Hexane	0.29	0.535	-0.035
Cyclohexane	0.43	0.386	0.006
N-Heptane	2.08	2.450	-0.053
N-Octane	4.50	4.654	-0.022
N-Nonane	4.60	4.654	-0.008
N-Decane	7.30	7.400	-0.015
N-Undecane	12.00	11.923	0.011
N-Dodecane	9.40	9.264	0.020
N-Tridecane	3.11	3.014	0.014
	100.0	100.0	0.0

TABLE XII

COMPARISON OF RICH OIL COMPOSITIONS OBSERVED AND CALCULATED FOR B24 TEST PERIOD

Component	Composition, Mole Per Cent		
	Observed	Calculated	Deviation, Moles
Carbon Dioxide	0.16	-0.029	0.032
Nitrogen	0.45	3.427	-0.511
Methane	25.60	28.230	-0.451
Ethane	10.90	9.709	0.205
Propane	16.00	13.543	0.421
I-Butane	2.73	2.265	0.080
N-Butane	6.50	5.226	0.219
I-Pentane	1.38	1.114	0.046
N-Pentane	1.57	1.186	0.066
2-Methylpentane	0.57	0.098	0.081
3-Methylpentane	0.17	0.052	0.020
N-Hexane	0.25	0.603	-0.061
Cyclohexane	0.09	0.276	-0.032
N-Heptane	1.20	1.868	-0.115
N-Octane	3.20	3.596	-0.068
N-Nonane	3.60	3.630	-0.005
N-Decane	5.80	5.830	-0.005
N-Undecane	9.50	9.460	.007
N-Dodecane	7.40	7.401	0.000
N-Tridecane	2.93	2.513	0.011
	100.00	100.00	0.00

TABLE XIII

COMPARISON OF RICH OIL COMPOSITIONS OBSERVED AND CALCULATED FOR B16 TEST PERIOD

Component	Composition, Mole Per Cent		
	Observed	Calculated	Deviation, Moles
Carbon Dioxide	0.16	-0.032	0.031
Nitrogen	0.00	2.700	-0.430
Methane	31.70	22.937	1.397
Ethane	10.90	10.839	0.010
Propane	13.30	15.176	-0.299
I-Butane	1.99	2.572	-0.093
N-Butane	4.10	5.754	-0.263
I-Pentane	0.48	1.198	-0.114
N-Pentane	0.56	1.275	-0.115
2-Methylpentane	0.15	0.104	0.007
3-Methylpentane	0.07	0.056	0.002
N-Hexane	0.21	0.647	-0.070
Cyclohexane	0.27	0.293	-0.004
N-Heptane	1.62	1.991	-0.059
N-Octane	3.80	3.824	-0.004
N-Nonane	3.90	3.861	0.006
N-Decane	6.20	6.200	0.000
N-Undecane	10.10	10.061	0.006
N-Dodecane	7.80	7.871	-0.011
N-Tridecane	2.69	2.673	0.003
	100.00	100.000	0.00

this criterion was used to close the material balance. In addition the sum of these deviations for all components was also zero since both sources employed the overall material balance constraint.

The disagreement between measured and calculated concentrations differed more for light hydrocarbons than for the heavy ends. In each case the largest deviation was in the methane concentration. This varied from 1.5 to 8.8 per cent. This deviation was compensated by deviations in the opposite direction for the other light components. For three cases the measured methane concentration was higher than the calculated value, while for the B24 case it was lower. These deviations served as a harbinger of problems to be encountered later.

A consistent set of oil analyses should result in only small deviations between the calculated and analytical rich oil compositions regardless which component initiates the heavy fraction.

The ratio of the heavy fraction in the lean oil to that in the rich oil is defined as α_j where the subscript, j, denotes the initial component in the heavy fraction. All components heavier than the jth component are included in this heavy fraction. For each test period these ratios are presented in Table XIV. For this base case octane was the initial component.

The selection of other initial components should have only a small effect on the ratio providing these compounds satisfy the constraint that they are present only in the oil streams. Figure 4 shows the variation in the α_j values for different initial components for the heavy fraction. The abscissa is the initial component of the heavy fraction, j. The heavy fraction extends from that component through

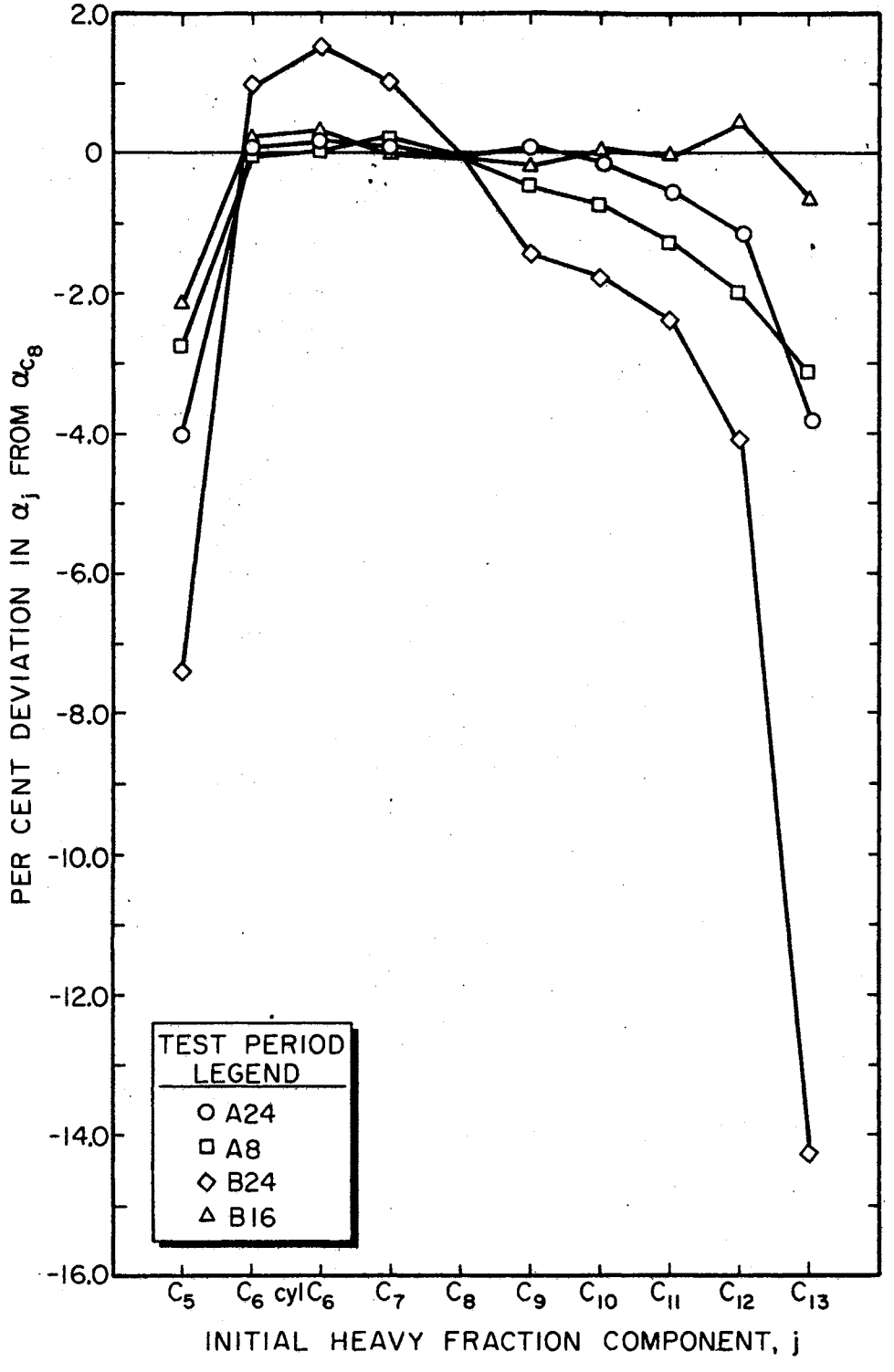

Figure 4. Variation in Heavy Fraction Ratio As More Components Are Included

C_{13}, the heaviest component. The per cent deviation in the heavy fraction ratio from that of the base case shown in Table XIV is the ordinate.

TABLE XIV

OCTANE PLUS FRACTION FOR LEAN OIL AND RICH OIL STREAMS FOR ALL TEST PERIODS

Test Period	Octane Plus Fraction		α_{C_8}*
	Lean Oil	Rich Oil	
A24	92.3	41.91	2.202
A3	92.3	40.91	2.256
B24	92.9	32.43	2.865
B16	92.9	34.49	2.694

*α_{C_8} ≡ Ratio of octane and heavier components in the lean oil to that in the rich oil.

The large deviation in the C_{13} end of the figure can be attributed to the uncertainty in analysis of a low concentration component. The ratio in this case is that of two small numbers and their uncertainties. As more components are included in the heavy fraction, stability increases. However, deviations greater than two per cent occurred with the inclusion of five-carbon compounds in the heavy fraction. Since pentane was present in the rich gas, it can not be included in the

heavy fraction for to do so would violate the constraints of equation 12. By including it in this figure the sensitivity of the equation to the constraint is shown.

For test periods A24, A8, and B16, the deviation from the base case oil rate ratio was less than one per cent of heavy fractions beginning with components in the C_6 to C_{10} range. This implies that an arbitrary choice of any of these heavy fraction ratios as a basis would make less than a one per cent change in the calculated rich oil rate.

For the B24 test period the variation was less than two per cent but more than double the deviation of the other test periods. This increased instability may have resulted from unstabilized operating conditions for that test period. The C_{8+} fraction does represent the median oil rate ratio for components in the C_6 to C_{10} range.

Although little deviation was introduced by the proposed method of closing the material balance regardless which component initiated the heavy oil fraction, considerable differences existed between analytical rich oil compositions and those calculated by component material balance. The uncertainty of the rich oil composition did not affect the calculated component recoveries any more than they affected the rich oil rate itself because component recoveries were taken as the difference between the rich gas and the dry gas component rates. The differences only served to indicate the degree that experimental errors entered this evaluation.

As a second evaluation of the experimental data, flash calculations were made for all streams of the four test periods. Using the component analysis, the measured temperature, and the measured pressure, flash calculations were made using vapor-liquid equilibrium K values

provided by the Chao-Seader correlation. For these calculations the gas streams should be at or above their dew point; the liquid streams should be at or below their bubble point.

Table XV presents the results from this analysis for each test period. For the A24 test period the lean oil was all liquid and the dry gas all vapor. On the bottom of the absorber the rich gas was below its dew point or 99.2 per cent vapor at flow conditions. These equilibrium calculations predicted the rich oil was only 98.7 per cent liquid.

TABLE XV

SUMMARY OF FEED AND PRODUCT STREAM CONDITIONS

Test Period	Stream Condition	Rich Gas	Lean Oil	Dry Gas	Rich Oil
A24	Temperature, °F	9	32	45	22
	Pressure	545	545	545	545
	L/F*	0.008	1.0	0.0	.985
A8	Temperature, °F	4	32	45	22
	Pressure	536	536	536	536
	L/F*	.008	1.0	0.0	.928
B24	Temperature, °F	11	34	47	24
	Pressure	575	575	575	575
	L/F*	0.001	1.000	0.0	.912
B16	Temperature, °F	11	34	47	23
	Pressure	565	565	565	565
	L/F*	0.002	1.0	0.0	.825

*Calculated fraction of the stream that is liquid.

For the A8 test period the lean oil and the dry gas were all liquid and gas respectively. The rich gas contained less than one per cent liquid. Comparable results were obtained for both the B24 and B16 test periods.

Results from the flash calculations of the rich oil stream deviated from expected values for all test periods. In each case, the rich oil was above its bubble point. For the A8 test period the rich oil was calculated to be 92.8 per cent liquid. Results from the B24 and B16 rich oil streams were 92.1 and 82.5 per cent respectively.

While the results from equilibrium flash calculations did not yield direct conclusions on their own, they did point to inconsistencies in the experimental data. The largest of these was the phase of the rich oil stream for all test periods. This stream was difficult to handle both physically and mathematically. The difficulty stemmed from the composition of stream. It was predominately a heavy oil saturated with light hydrocarbons and only small amounts of intermediate components. With such a wide range of boiling points, the stream was very sensitive to the operating temperature and pressure. Thus, any rise in temperature or drop in pressure would have changed the near equilibrium rich oil into a two phase mixture.

Such deviations as found in the rich oil phase calculations may have been attributed to: (1) experimental measurements of the temperature and pressure; (2) stream analysis including sampling technique and component analyses; or (3) calculation procedures used to predict equilibrium values.

Additional equilibrium calculations were made for the rich oils at the measured pressure to determine the bubble point temperature and,

likewise, at the measured temperature to determine the bubble point pressure. Results from these calculations are summarized in Table XVI. The operating conditions were the closest to bubble point conditions for the A24 test period. In this case the difference between measured temperature and bubble point temperature at the measured pressure was 11°F. The calculated bubble point pressure was 33 psi above the experimental value. The deviations for the other test periods were greater than these.

TABLE XVI

CALCULATED BUBBLE POINT CONDITIONS FOR THE RICH OIL SAMPLES

Test Period	Measured Conditions		Calculated Bubble Points	
	Temperature °F	Pressure psia	Temperature at Measured Pressure	Pressure at Measured Temperature
A24	22	545	11	578
A8	22	536	1	693
B24	24	575	-19	759
B16	23	565	-26	937

The uncertainties of temperature and pressure measurements were estimated to be 5°F and 5 per cent or 25 psi respectively. Uncertainties of this magnitude cannot alone explain the deviations in the bubble point conditions.

The second factor influencing the bubble point evaluation was the sample analysis for the rich oil stream. First examine the sampling technique itself. The sample was obtained from a drain valve for a sight glass used to determine the liquid level in the bottom of the absorber. The average liquid head on the sight glass was between one and two feet. The oil in the sight glass had no froth as it was isolated from the dynamic unit. The rich oil coming from the tower to the sample bomb did not have the equivalent settling time and may have had entrained gas from the froth above the rich oil. This froth entrainment would produce samples whose analysis would have high concentrations of light ends because the sample actually was taken as a two phase mixture rather than the saturated rich oil product.

The degree of entrainment would vary as the liquid level varied. At a higher liquid level, less entrainment would be expected because more time was available for separation of the phases. For each test period the liquid level in the absorber was observed for relative change during a test period but the actual level was not recorded.

So, gas entrainment in the rich oil sample would cause bubble point calculations to predict lower temperatures and higher pressures than observed. The entrainment hypothesis would also explain the difference between the rich oil composition obtained by sample analysis and those obtained by individual component material balances.

These sample analyses were carried out by Phillips Petroleum Company in Bartlesville, Oklahoma. Check analyses were obtained for all liquid samples when the discrepancies between calculated compositions and reported analytical results were observed. The repeated analyses

were within reasonable limits on all major components, less than 0.1 mole per cent.

The vapor-liquid equilibrium constants used in these calculations were predicted by the Chao-Seader correlation. Individual components were identified for the lighter portion of the oil. Eight carbon and heavier components defied complete identification and they were reported only by carbon number and per cent aromatics. These components were grouped to include compounds of several carbon numbers. Properties for these pseudo-compounds were generated by a physical properties subroutine contained within the program.

Components of this range fall at the limit of the Chao-Seader correlation with reduced temperatures below 0.5. For the operating conditions of these absorbers, all components with critical temperatures above 510°F have reduced temperatures below 0.5. This includes all components heavier than heptane. In spite of being out of range, the Chao-Seader correlation was still employed as a consistent, readily available source of vapor-liquid equilibrium data. Any large errors due to heavy component description could be adjusted by manipulating the calculated physical properties of the pseudo-components. In addition the vapor-liquid equilibrium constants for these components were not critical in evaluating heavy component recoveries. Because they were very small numbers, their absorption factor was large and they left wholly in the rich oil stream.

The consistency of the K-values employed to flash each of the rich oil samples was checked. The log K was linear with respect to the square of the critical temperature for all components except methane. The K-values required to fall in line with the other components were

50 to 100 per cent higher than those predicted by the Chao-Seader correlation. Methane equilibrium values that large would have resulted in additional vaporization of the rich oil sample. The results from this consistency test indicated that the problem incurred with the rich oil streams was not the result of inconsistency of K-value data.

In the absence of exact analytical procedures and experimental vapor liquid equilibria data, both the chromatographic analysis and the application of the Chao-Seader correlation represented inprovements over first order approximations generally employed in absorber calculations.

However, the strong dependence of K-values of the heavy components on temperature and the incomplete resolution of components in the octane to tridecane range inhibited rigorous bubble and dew point calculations.

A third consistency check on the material balance around each absorber can be made by employing heat balances. For convenience, the standard heat balance equation--heat in equals heat out--has been arranged as follows.

$$Q = (H_{DG} + H_{RO}) - (H_{RG} + H_{LO})$$

In this equation H represents the enthalpy of the stream indicated by the subscript. The first set of terms is the product enthalpy and the second is the feed. The deviation Q includes both sensible heat entering the absorber and uncertainty of the experimental data. The NGPA K and H Value Computer Program provided the stream enthalpies at measured conditions.

In Table XVII the summary of all heat balance calculations is presented. These calculations have been based on a rich gas feed rate of 100 moles per hour. Units for the stream enthalpies are 1000 Btu per hour.

TABLE XVII

SUMMARY OF HEAT BALANCES

Test Period	Enthalpy, M Btu/hr				Q	Q/H_{feed} %
	Dry Gas	Rich Oil	Rich Gas	Lean Oil		
A24	347.2	-16.3	337.6	-12.6	6.4	2.0
A8	346.4	-16.5	338.0	-12.5	4.4	1.4
B24	332.9	-11.4	338.5	-11.5	-5.5	-1.7
B16	337.1	- 5.2	338.5	-11.4	4.7	1.4

For the A24 test period the deviation was 6.4 Btu/hr or 2.0 per cent of the feed enthalpy. For both the A8 and B16 test periods the deviations were 1.4 per cent of the feed enthalpy. The deviation for the B24 test period was negative indicating heat leaving the system. This must indicate an error in the material balance or the enthalpy calculations because the absorbers were operated below ambient temperature. This deviation was -5.5 M Btu/hr or -1.7 per cent of the feed enthalpy.

All deviations have been presented as sensible heat lost or gained from the system. There was no way to separate the exact amount of heat gained by the absorbers from surroundings from that introduced by uncertainties. However, from Appendix E, approximately 0.5 M Btu/hr would be gained by an absorber of the size encountered and operated at the measured conditions. The remainder of the deviation, Q, must arise from uncertainties in the material balance and enthalpy calculations. These uncertainties more than overshadow the sensible heat gained by the system and eliminate any need to correct for the heat leaks.

As a check on the enthalpy source, a second heat balance around each of the absorbers was made using Kellogg enthalpies (5). The results from these balances were as follows for the heat entering the absorber as a per cent of the feed enthalpy: A24-- -0.5; A8-- -3.6; B24-- -4.1; and B8-- -5.1 per cent. In each case the deviation showed heat leaving the system. This deviation, approximately five per cent, was interpreted as the order of magnitude of the uncertainty in the overall balances of the systems.

From this evaluation of the data one fact becomes apparent--the rich oil stream was the major source of uncertainty for all four test periods. First, the composition calculated by component material balance differed up to eight per cent from the analytical composition. Second, the equilibrium phase calculations predicted the rich oil to be from 2 to 18 per cent vapor. The accurate compositions of these rich oil streams were not directly required for the comparison with stagewise calculations. They were required before those comparisons were undertaken to evaluate the rich oil and rich gas rates. The data evaluation also pointed out some of the problems encountered when

when research grade data were to be obtained from plant scale equipment.

Comparison with Stagewise Calculations

Once consistent experimental data had been established for each absorber test period, a comparison of actual results with those predicted from theoretical models was undertaken. An ideal tray model was used to predict product rates, temperatures, and concentrations for specified operating conditions.

The effectiveness of the actual absorber was determined by comparison with predicted results for various numbers of equilibrium stages. Solutions used in this evaluation were rigorous tray-by-tray calculations for an ideal tray absorber. These solutions were obtained using the Sujata convergence technique (22) programmed by Spear (21). The specifications required to uniquely describe an absorber for this program were rate, temperature and composition of both feed streams; the operating pressure of the absorber; and the number of theoretical stages. Of these requirements, all were directly measured except for the rich gas rate and the number of theoretical stages. The rich gas rate was calculated from material balance procedures, while the number of theoretical stages remained the major adjustable parameter to determine the effectiveness.

A macroscopic point of view for effectiveness was taken because only boundary variables of the unit were monitored and insufficient data were obtained for a microscopic efficiency study. The effectiveness was principally the number of theoretical stages required to reproduce the operating conditions of the actual unit. In addition to

the number of theoretical stages, several other parameters were investigated to more completely reproduce the operating conditions. These variables affected calculated results through the evaluation of thermodynamic properties. They were operating pressure of the absorber, characterization of the heavier components, and source of the thermodynamic properties themselves.

In order to match calculated values with experimental values a set of target values was defined for each test period. Included in this set of parameters were both product temperatures, the dry gas rate, and the concentration of the distributed components in the dry gas stream. Methane, ethane, and propane constituted these distributed components. The rich oil rate was omitted as it was directly coupled to the dry gas rate. Similarly, the concentrations of the light hydrocarbons in the rich oil were not included as target parameters.

The choice of the number of theoretical trays was arbitrary. The eight tray model was first investigated since it was about 30 per cent of the total number of trays, the nominal efficiency of absorbers. Four trays were employed to yield results for fewer trays while 16 and 24 were investigated to cover the possibilities up to 100 per cent efficiency. Had the results of one of the other choices appeared to closely match experimental values then that particular number of trays would have been used in further investigation.

The product stream temperatures approached the experimental values when 16 theoretical trays were employed. For fewer trays the dry gas temperature was below the experimental value while the rich gas temperature was above the experimental value. This resulted from lower total absorption and closer physical relation of the product streams.

As the number of trays increased, the dry gas temperature rose 6°F while the rich oil temperature dropped only 2°F.

The overall absorption as indicated by the difference between the rich gas and the dry gas rates increased with increasing number of trays. However, with 24 theoretical stages, the model could not predict as much absorption as was actually obtained for the operating unit. The relative contribution of theoretical stages on the total absorption was indicated by these results where a 6-fold increase in the number of theoretical stages produced only 5 per cent change in the total absorption amounting to only 0.4 per cent of the measured dry gas rate.

Just as the increase in the number of theoretical trays did not provide as much total absorption as experimentally encountered, neither did it produce the component recoveries of the actual absorber. In all cases the methane concentration in the dry gas stream was below analytical results. This indicated insufficient recovery of ethane and the heavier components of the rich gas stream. For the 16 tray model the ethane concentration was in good agreement with experimental values. This left the propane and heavier components to account for the unrecovered portion. Since all of the butane and heavier components were completely recovered, propane remained as the unrecovered portion. This was substantiated in the results shown in Figure 5. The propane recovery could not be accomplished solely by increasing the number of theoretical stages.

For the A24 test period, a match of product temperatures was reached near 16 theoretical stages. However, based on overall and individual component recoveries, a 24 theoretical tray absorber would not absorb as much lightends as the 24 actual tray plant unit. Thus,

TABLE XVIII

SUMMARY OF ABSORBER MODEL SOLUTIONS BASED UPON A24 TEST PERIOD

Trays	Dry Gas					Rich Oil	
	Temperature °F	Rate Moles	Composition, Mole Per Cent			Temperature °F	Rate Moles
			Methane	Ethane	Propane		
Experimental 24	45.0	92.323	86.150	6.417	1.553	22.0	14.062
4	40.6	92.847	85.662	6.456	1.886	23.7	13.539
8	40.7	92.545	85.896	6.423	1.751	22.0	13.841
16	45.8	92.507	85.921	6.420	1.741	21.4	13.880
24	46.6	92.472	85.911	6.425	1.751	22.7	13.911

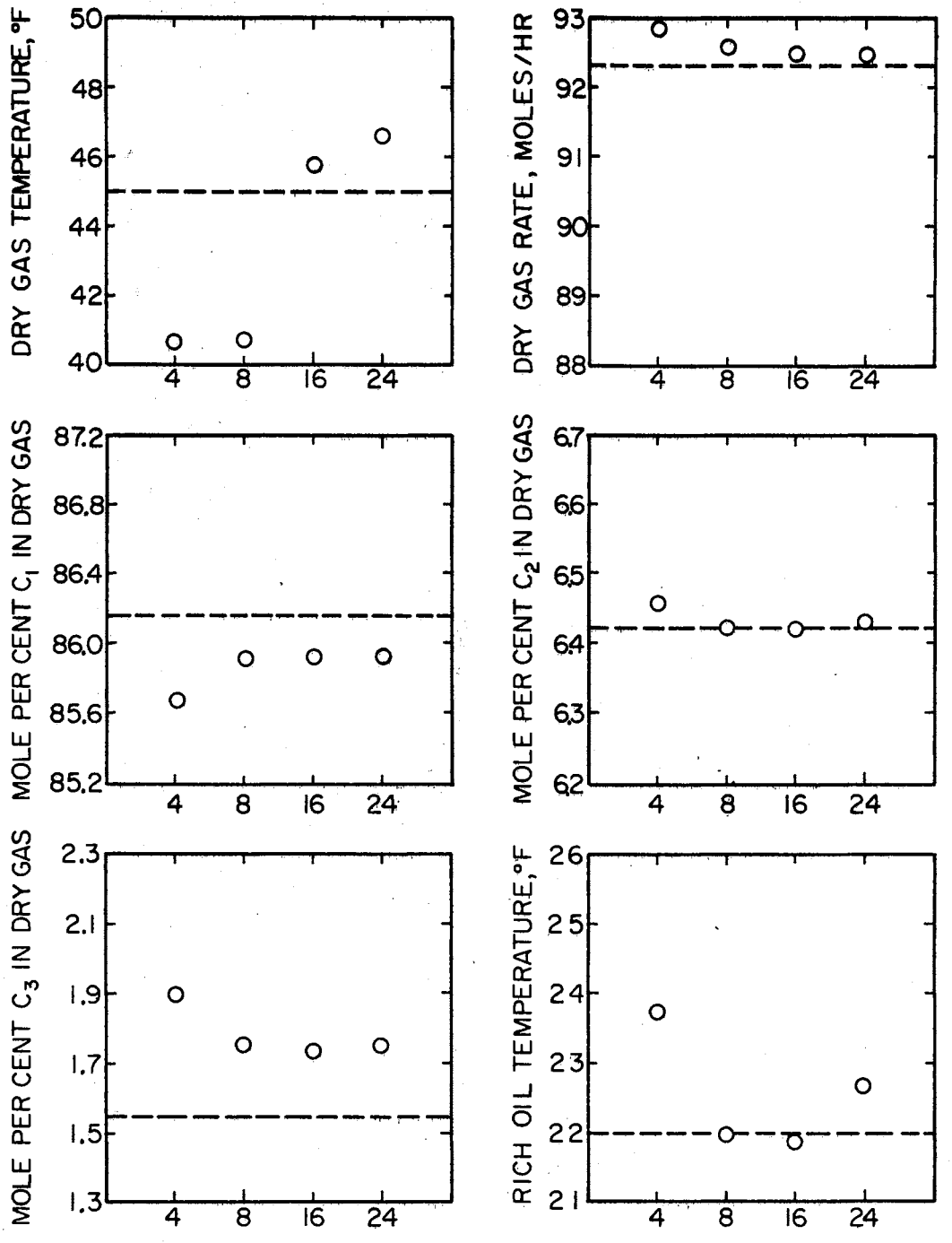

Figure 5. A Comparison of A24 Test Period Results With Calculated Values as the Number of Theoretical Stages Is Increased

change brought by variation in the number of theoretical stages was not sufficient to reach the experimental recoveries.

Similar calculations were made for the A8, B24, and B16 test periods. Results from these calculations are presented in Tables XIX through XXI and compared with experimental values in Figures 6, 7, and 8.

For the A8 test period, four theoretical trays produced a solution with too little absorption. This fact was evidenced in each of the six sections of Figure 6. The dry gas rate was one per cent high, the dry gas temperature was $5^{o}F$ low. The methane concentration was too low while the ethane and propane concentrations were too high. All of these facts indicated lower absorption than actually encountered during the test period.

By increasing the number of theoretical trays to eight, doubling the initial value, increased recovery was noted. The improved results did not approach experimental values sufficiently to merit calculations with more theoretical trays.

Similar results were reported for both the B24 and B16 test periods--overall recoveries less than experimentally determined ones. In both cases, an increased number of trays produced results closer to experimental values. However, these contributions to the recoveries were again insufficient to match the recoveries of the experimental results.

In addition to the number of ideal stages, other input variables for the tray-by-tray program were investigated to determine their effect on the calculated solutions. Variables included in this investigation were column operating pressure, characterization of the lean oil, and source of the thermodynamic properties. The magnitude of these effects

TABLE XIX

SUMMARY OF ABSORBER MODEL SOLUTIONS BASED UPON A8 TEST PERIOD

Trays	Dry Gas					Rich Oil	
	Temperature °F	Rate Moles	Composition, Mole Per Cent			Temperature °F	Rate Moles
			Methane	Ethane	Propane		
Experimental 8	45.0	91.985	86.290	6.273	1.372	22.0	14.395
4	40.1	92.952	85.615	6.505	1.888	22.8	12.424
8	43.3	92.644	85.816	6.476	1.775	21.8	13.732

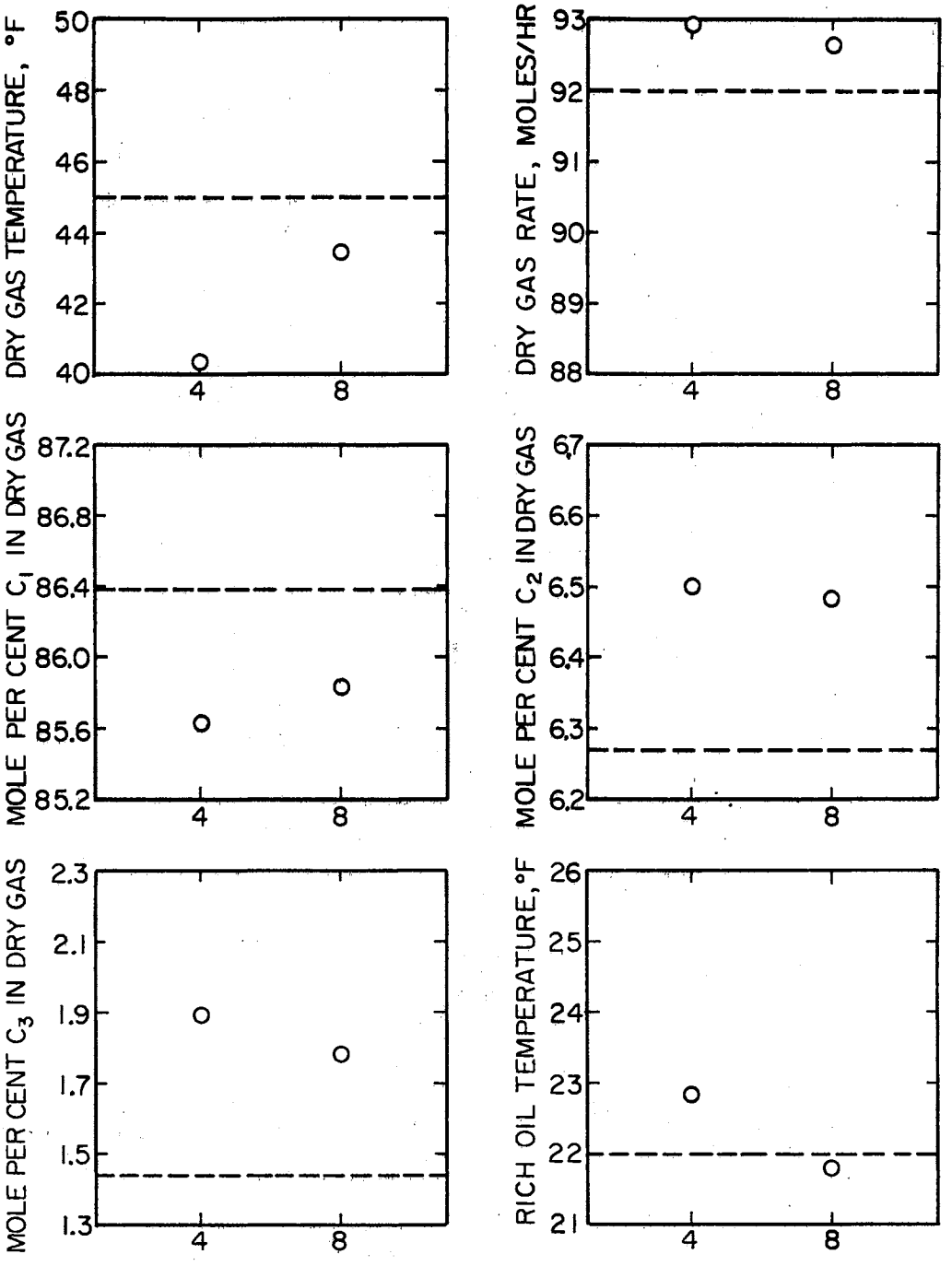

Figure 6. A Comparison of A8 Test Period Results With Calculated Values as the Number of Theoretical Stages Is Increased

TABLE XX

SUMMARY OF ABSORBER MODEL SOLUTIONS BASED UPON B24 TEST PERIOD

Trays	Dry Gas					Rich Oil	
	Temperature °F	Rate Moles	Composition, Mole Per Cent			Temperature °F	Rate Moles
			Methane	Ethane	Propane		
Experimental 24	47.0	88.830	86.434	6.380	1.524	24.0	17.160
4	41.1	92.676	85.326	6.590	1.990	24.7	13.316
8	44.3	92.341	85.542	6.558	1.869	23.6	13.650
16	47.3	92.224	85.619	6.546	1.824	23.2	13.770
24	47.1	92.247	85.608	6.553	1.834	23.6	13.744

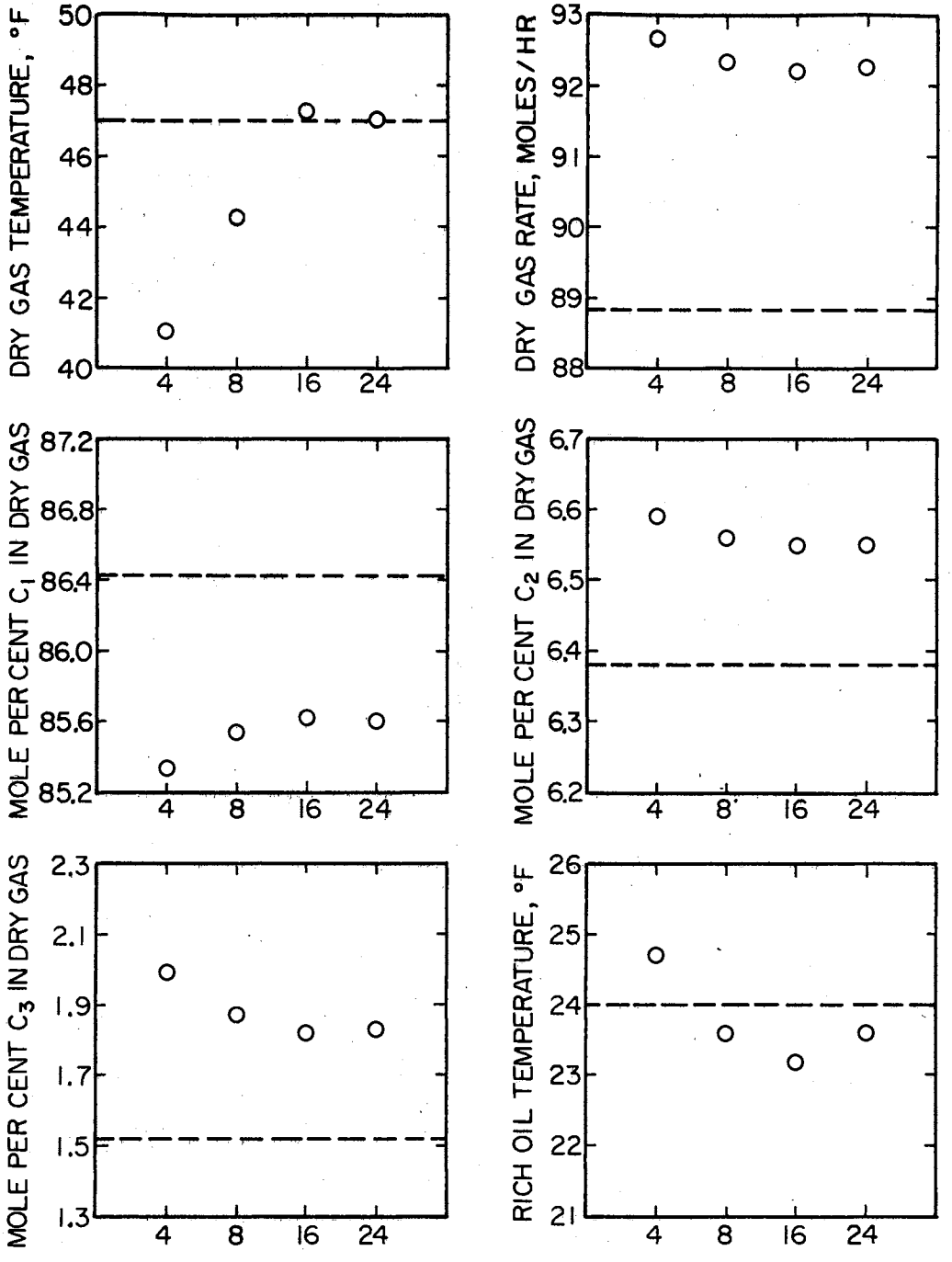

Figure 7. A Comparison of B24 Test Period Results With Calculated Values as the Number of Theoretical Stages Is Increased

TABLE XXI

SUMMARY OF ABSORBER MODEL SOLUTIONS BASED UPON B16 TEST PERIOD

Trays	Dry Gas					Rich Oil	
	Temperature °F	Rate Moles	Composition, Mole Per Cent			Temperature °F	Rate Moles
			Methane	Ethane	Propane		
Experimental 16	47.0	89.978	86.652	6.230	1.399	23.0	15.940
4	41.0	92.822	85.280	6.609	2.018	24.6	13.096
8	44.3	92.498	85.489	6.580	1.903	23.5	13.419
16	47.2	92.380	85.567	6.568	1.858	23.1	13.538

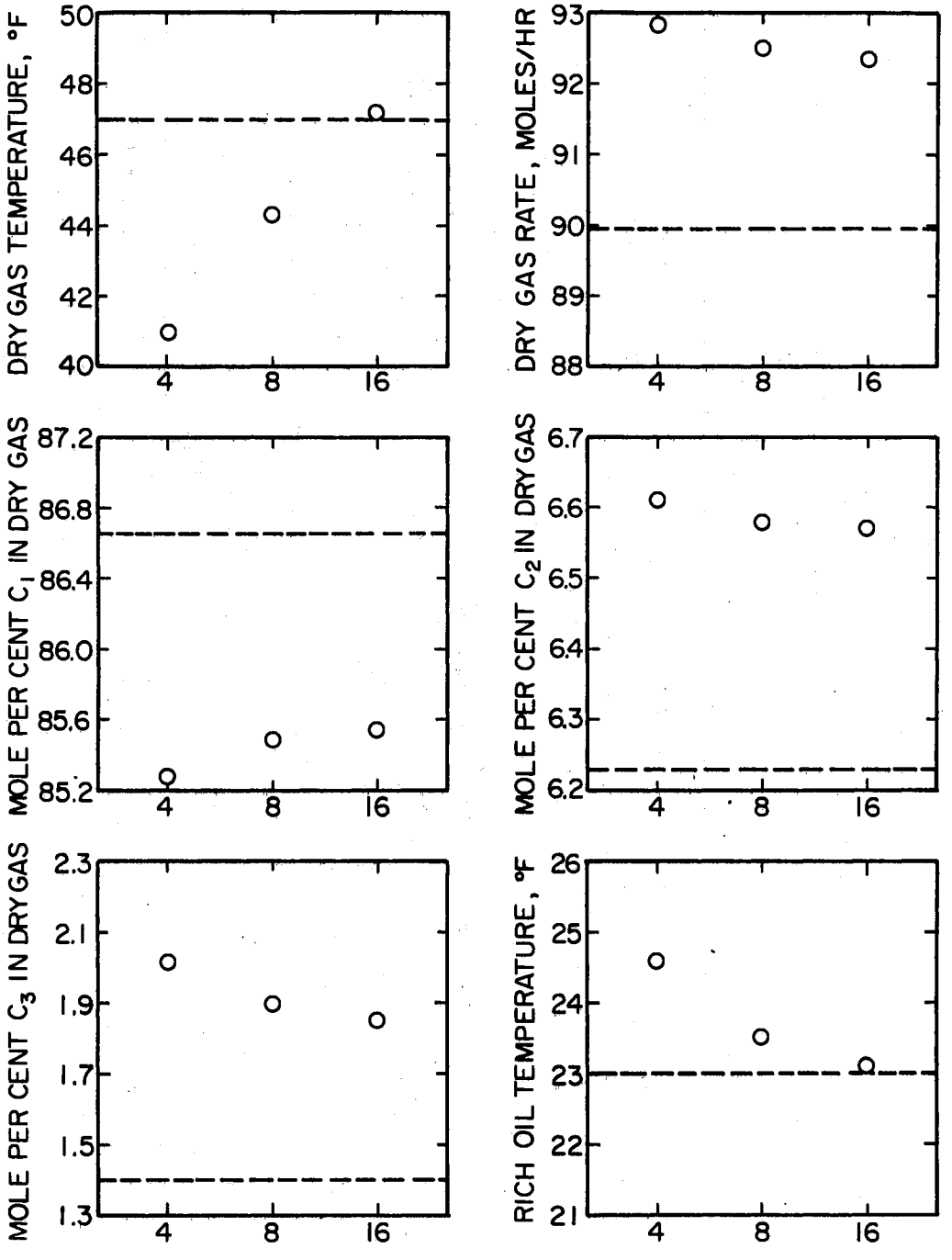

Figure 8. A Comparison of B16 Test Period Results With Calculated Values as the Number of Theoretical Stages Is Increased

must be developed before any generalization can be made for the uncertainty of the experimental data.

The uncertainties of pressure measurement were of two types, one major--an error in the absolute measured value itself--and one minor--pressure drop per tray of the column. The pressure drop per tray was assumed to be zero by the computer program used for these calculations. By making calculations at different pressures not only the effect of moderate errors in the measured column pressure but also the contribution due to stagewise pressure drops were investigated. All of these variations in the pressure affect the solution through the evaluation of the equilibrium constants and enthalpies.

A test case was made using the A24 test period as the basis of comparison. Calculations were made at pressures 10 psi above and below the measured value of 545 psia. Eight theoretical trays were used throughout this evaluation. Results from these calculations are presented in Table XXII along with the experimental values and the results of calculations made at the measured pressure.

Only small changes were observed in the solutions and these results favored the elevated pressure. For the 555 psia solution, the total recovery indicated by the dry gas rate was approaching the experimental value. Overall, this solution more nearly approximated the experimental values than the solution at the reported pressure regardless of the number of trays employed. This improvement, however, was not sufficient to provide component recoveries comparable with experimental ones. By paralleling these results with those in Figure 5, even the combined effects of increased pressure and more trays would not bring these recoveries to the experimental level.

The difference between recoveries at various pressures was the result of changes in the equilibrium value for the lighter components due to pressure. As Figures 9, 10, and 11 show, the equilibrium constants for methane, ethane, and propane decrease with increased pressure. These values were obtained from the equilibrium flash calculations performed on each stage of the various solutions. Since all of these uncertainties affect the component recoveries through the equilibrium constants, the variation they produced in the constants was presented for further comparisons. For the 1.8 per cent change in the operating pressure, the methane K-value was changed about 1.7 per cent. The ethane and propane K-values were changed 1.4 and 1.0 per cent.

TABLE XXII

RESULTS FOR AN EIGHT TRAY MODEL OF THE A24 ABSORBER AT VARIOUS PRESSURES

Variable	Pressure, psia			
	545*	535	545	555
Dry Gas				
Temperature, ^{o}F	45	40.7	40.7	40.7
Rate, moles/hr	92.323	92.596	92.545	92.396
C_1, mole per cent	86.150	85.863	85.896	85.935
C_2, mole per cent	6.417	6.439	6.423	6.403
C_3, mole per cent	1.553	1.771	1.751	1.728
Rich Oil				
Temperature, ^{o}F	22	22.3	22.0	22.3

*Experimental values.

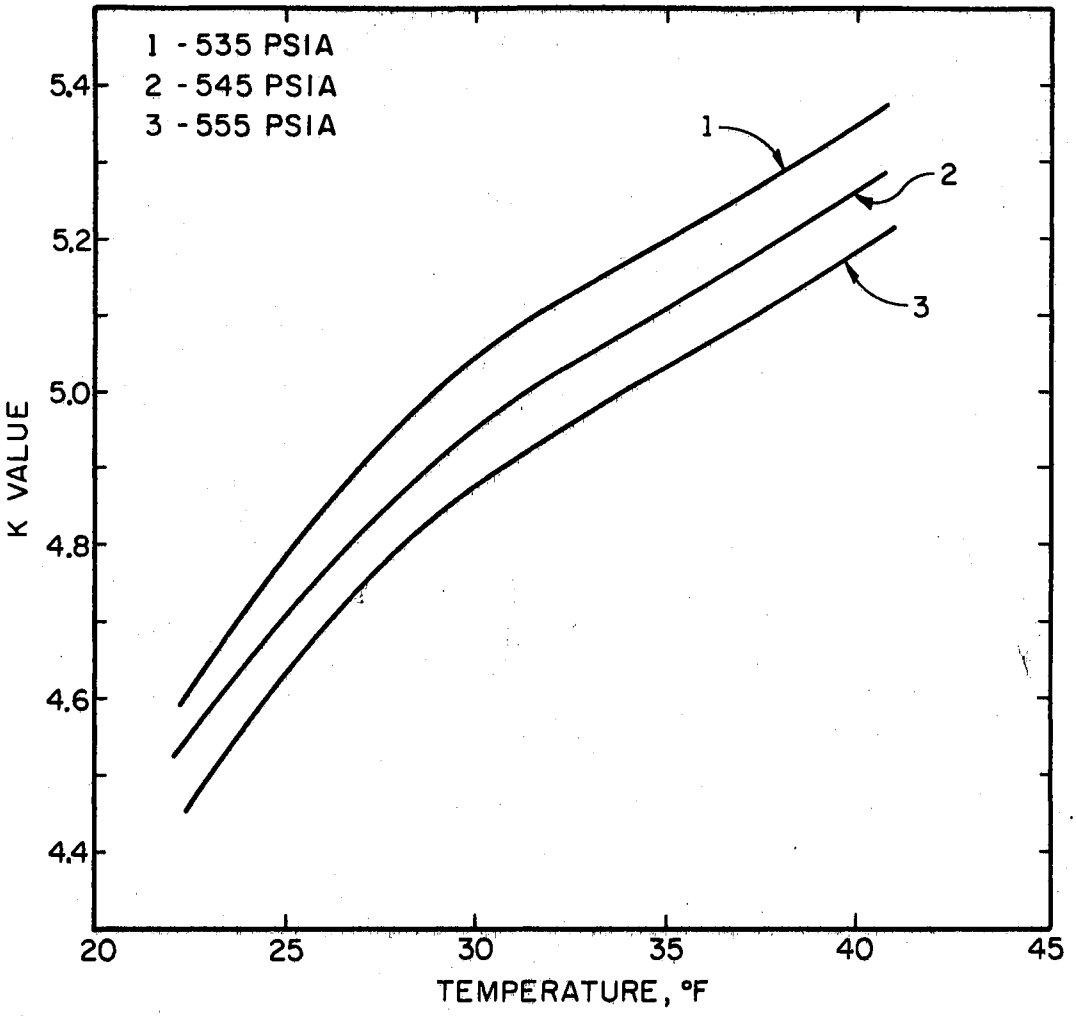

Figure 9. Pressure Dependence of Methane Equilibrium Values for A24 Test Period

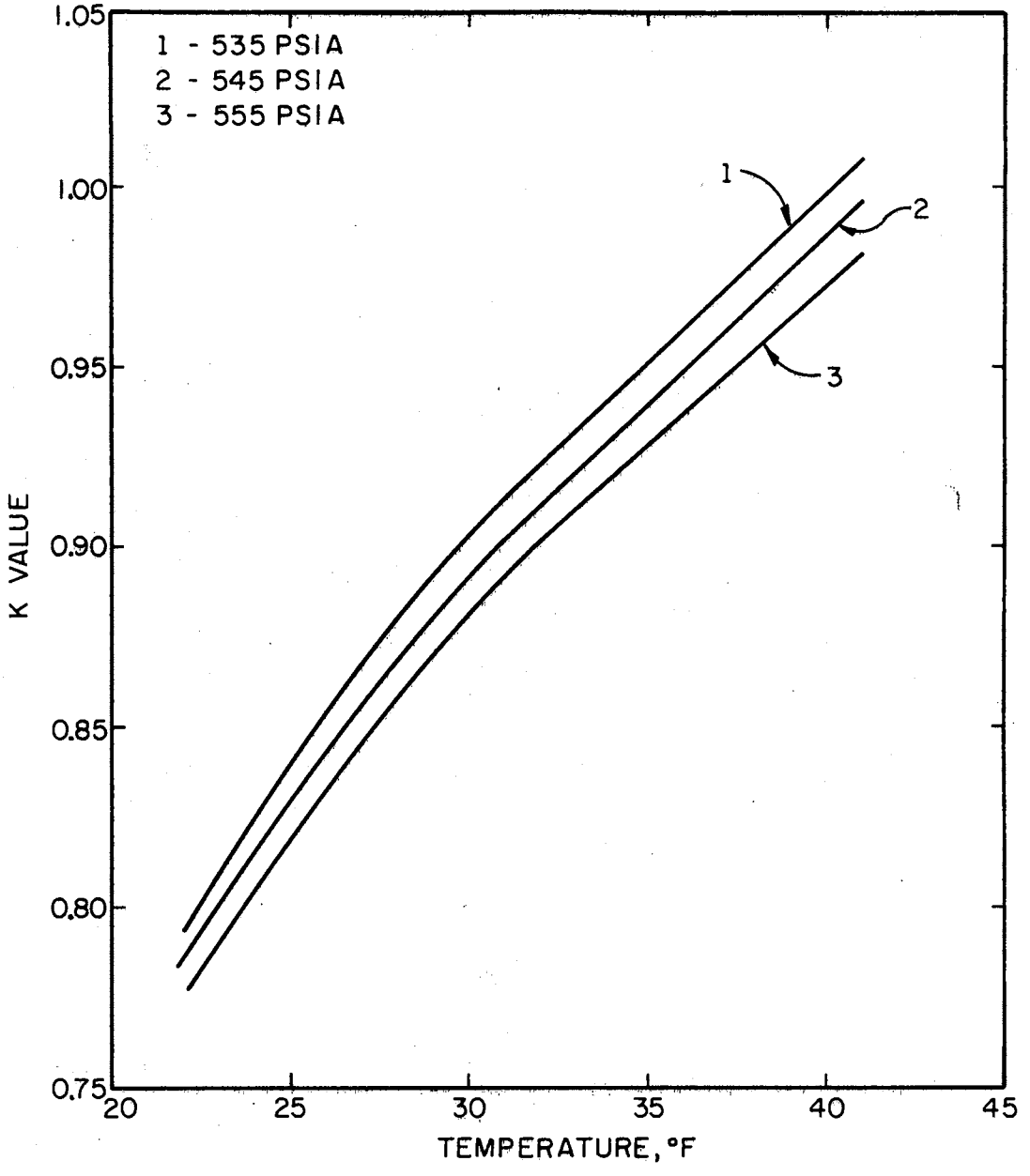

Figure 10. Pressure Dependence of Ethane Equilibrium Values for A24 Test Period

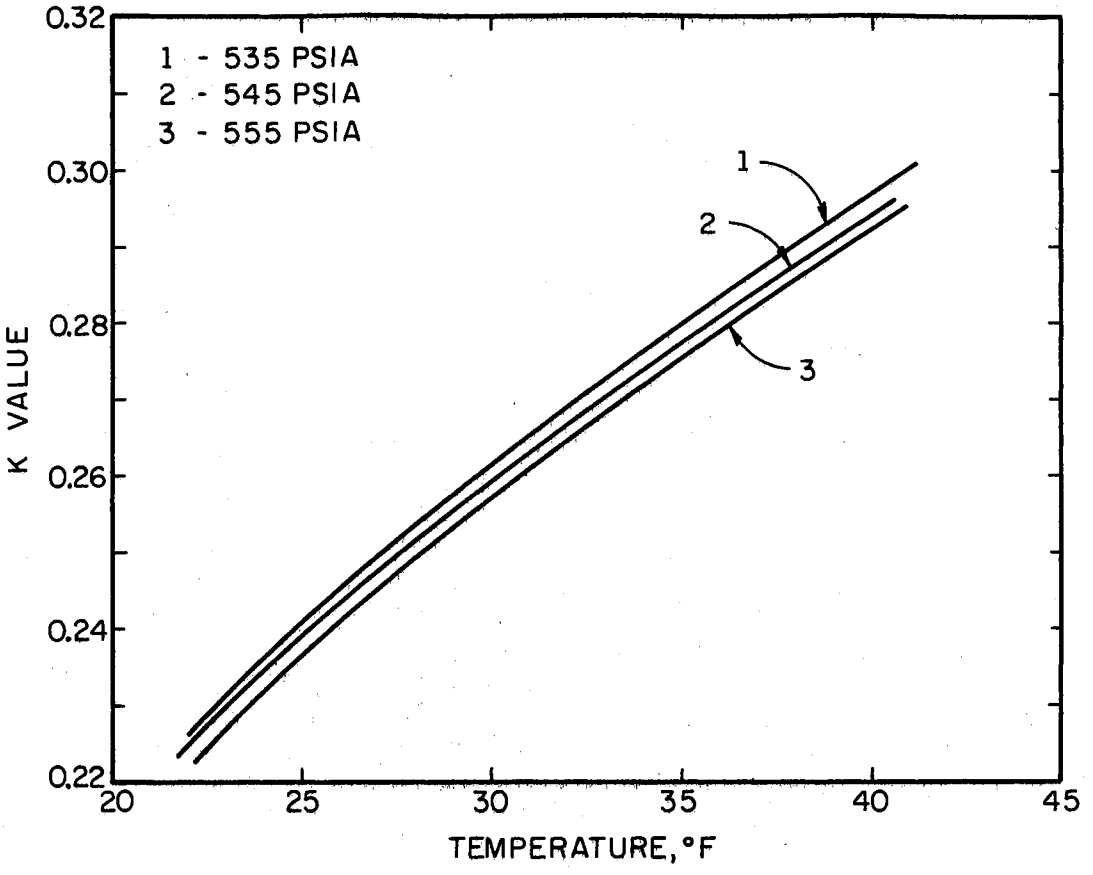

Figure 11. Pressure Dependence of Propane Equilibrium Values for A24 Test Period

A second indirect factor affecting the absorber model solutions was the description of the lean oil. A complete component identification of the heavy fraction was beyond the range of both analytical and computational capabilities. The analysis, however, did provide carbon number distribution and paraffin-aromatic ratio for the oil samples. This description directly affected the estimated molar density required to determine the lean oil molar feed rate. Indirectly, the type and amount of components comprising the absorption oil affected the calculation of vapor-liquid equilibrium constants.

The equilibrium constants for the heavy components had no significant effect on their recoveries because their absorption was complete. The absorption factor for these components was large due to the small K-values. Order of magnitude changes in their equilibrium values resulted in no change in recovery.

The characterization of this portion of the absorption oil was important in determining the vapor-liquid equilibrium constants for the light hydrocarbons. Figures 12, 13, and 14 present the relative dependence of methane, ethane and propane K-values on three different characterizations of the heavy oil fraction. These values were obtained directly from absorber calculations with the imcorporated Chao-Seader procedure.

The largest values for each component were predicted using three pseudo-components to represent all compounds with six or more carbon atoms. The intermediate values were predicted when those components were divided by carbon number and ten per cent aromatics were included in the description. The third set of equilibrium values was included to indicate the importance of complete characterization of the oil.

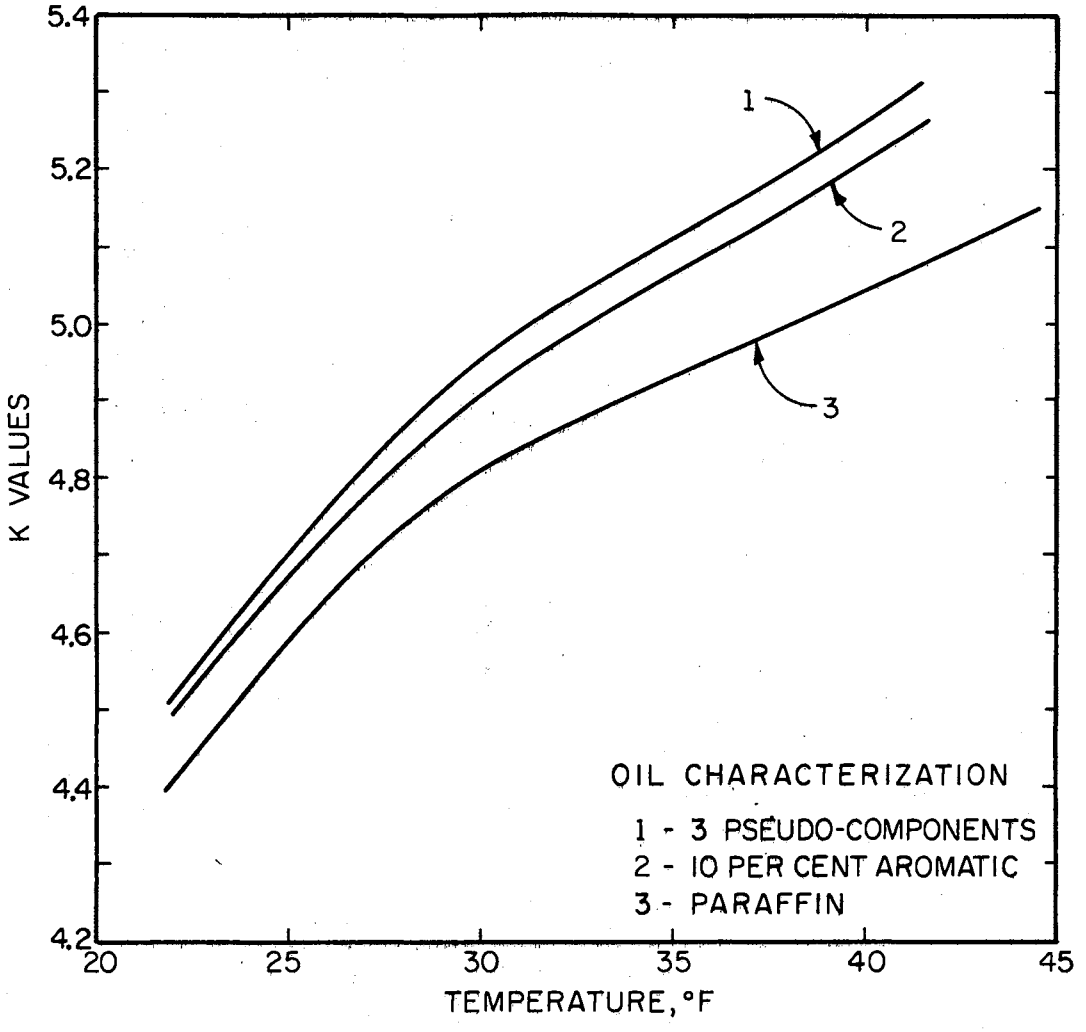

Figure 12. Composition Dependence of Methane Equilibrium Values for A24 Test Period

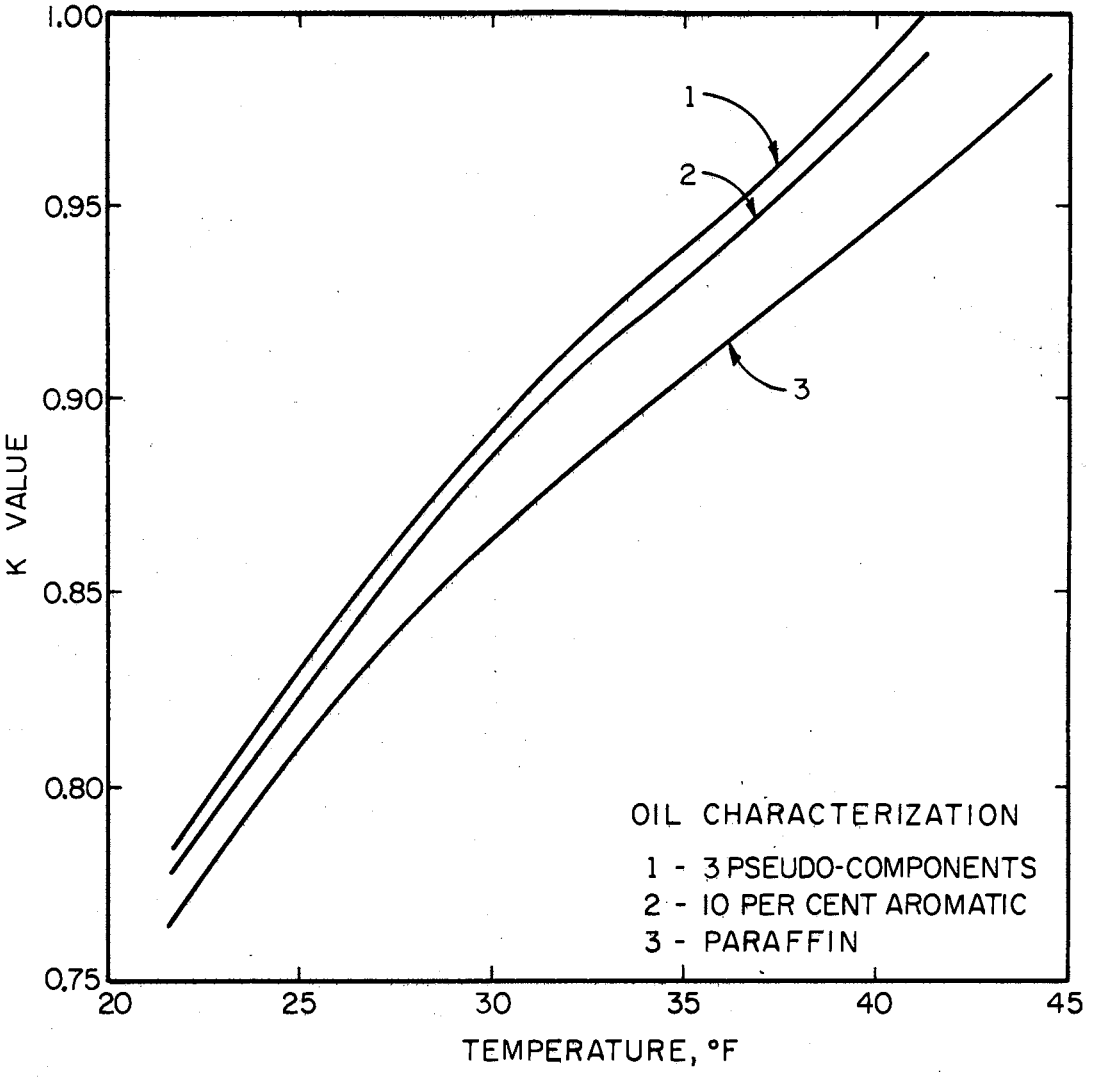

Figure 13. Composition Dependence of Ethane Equilibrium Values for A24 Test Period

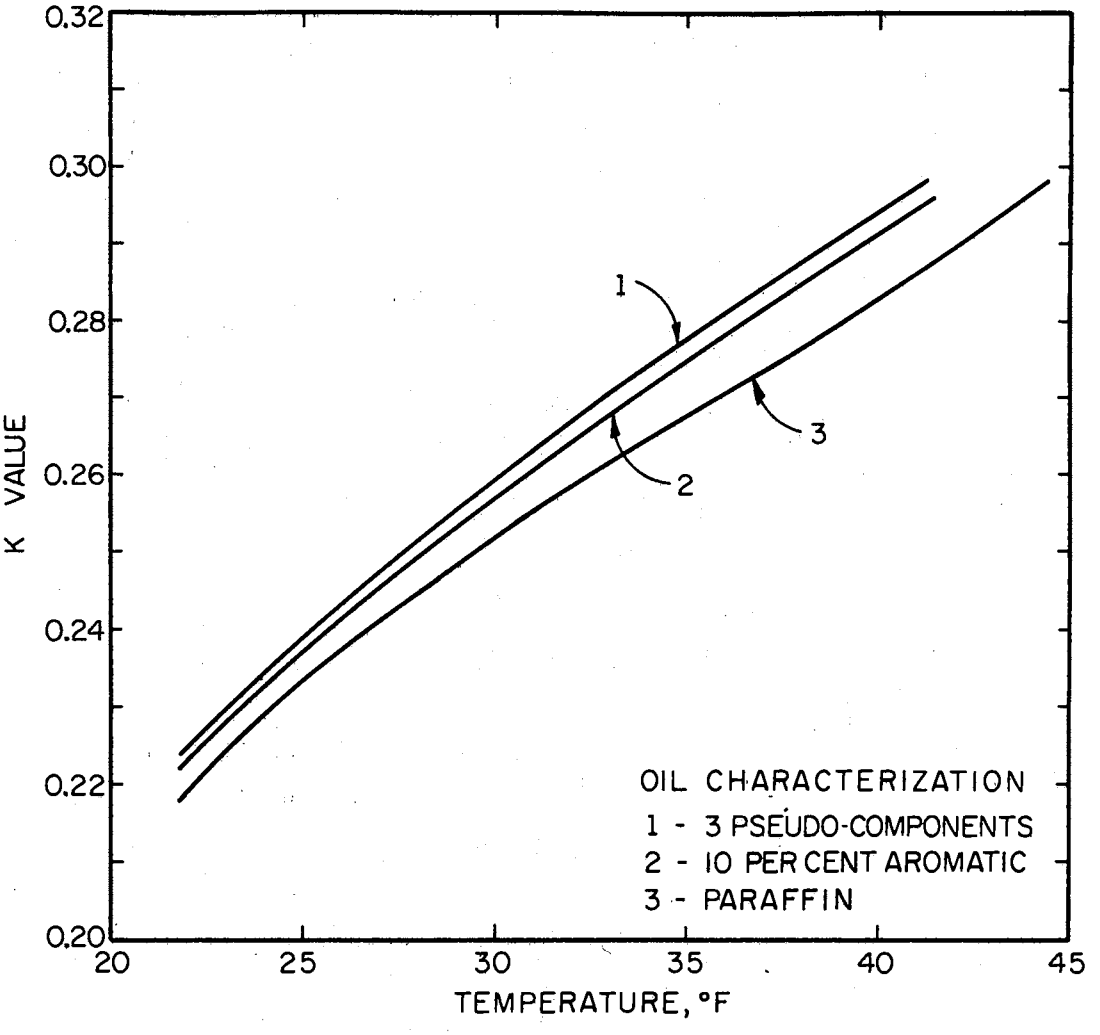

Figure 14. Composition Dependence of Propane Equilibrium Values for A24 Test Period

For this case all six carbon and heavier components were simply classified as normal paraffins with the same chain length.

All equilibrium values for these figures were obtained from results of the Sujata tray-by-tray program with the Chao-Seader correlation included. The absorber specifications were based upon the A24 test period at 545 psia and eight theoretical trays. Produce compositions, rates, and temperatures predicted by these calculations are summarized in Table XXIII.

TABLE XXIII

RESULTS FOR AN EIGHT TRAY MODEL OF THE A24 ABSORBER WITH DIFFERENT OIL CHARACTERIZATIONS

Variable	Characterization			
	Experimental	3-Pseudo-Components	10 Per Cent Aromatic	Paraffin
Dry Gas				
Temperature, °F	45	40.7	40.8	40.8
Rate, moles/hr	92.323	92.545	92.521	92.346
C_1, mole per cent	86.150	85.896	85.401	85.974
C_2, mole per cent	6.417	6.423	6.416	6.386
C_3, mole per cent	1.553	1.751	1.740	1.690
Rich Oil				
Temperature, °F	22	22.0	22.0	22.2

The light hydrocarbon K-values obtained using the complete carbon number breakdown to describe the oil were approximately one per cent lower than those predicted for the three pseudo-component oil description. Results from absorber solutions obtained using the paraffin description had K-values 2.5 to 4.0 per cent lower than those of the 3 component description. These additional characterizations of the oil were employed to illustrate the effect of the description of the absorber oil had on the K-values of the light hydrocarbons. No inference is intended that the heavier components should have been characterized as paraffins, but rather the description of the heavier portion of the absorber oil should be complete before attempting exact mathematical modeling.

A recent report by the NGPA (24) indicated the same large change in K-values for the light hydrocarbons with the changes in the oil composition. Data from four systems described in Table XXIV were presented in that report. Although none of these absorber oils were similar to the 150 molecular weight oil employed during these tests, the K-values for these systems were compared to those calculated for the plant tests.

For the typical Gulf Coast absorber oils, A and B, the methane K-values were five per cent above those calculated for these tests. The ethane and propane K-values were below calculated ones by 12 and 15 per cent. For the highly aromatic absorber oil, C, the differences were 22, -4, and -15 per cent for methane, ethane, and propane. K-values for the highly napthenic oil system, D, differed from predicted values by 12, -18, and -22 per cent. While the systems studied in the NGPA report were not comparable to the Blackwell unit, they did further

indicate the importance of knowing the absorber oil makeup and having experimental data to back up vapor-liquid equilibrium calculations.

TABLE XXIV

DESCRIPTION OF FOUR REAL ABSORBER OILS

Absorber Oil	Paraffin	Napthene	Aromatic	Mol. Wt.
A Typical Gulf Coast	45.7	40.2	12.2	103
B Typical Gulf Coast	52.2	35.6	12.2	130
C Highly Aromatic	34.6	32.2	33.1	122
D Highly Napthenic	33.0	57.6	9.4	113

Source: Wilson, G. M., and S. T. Barton, "K-Values in Highly Aromatic and Highly Napthenic Real Oil Absorber Systems." Research Report-2 Natural Gas Processors Association, Tulsa, Oklahoma, March, 1971.

A third indirect variable investigated was the equilibrium values themselves. Three sources provided vapor-liquid equilibrium constants for the tray-by-tray program. Primarily, equilibrium values were predicted from the Chao-Seader correlation contained in the absorber program. Secondary sources of equilibrium values were two computer programs--the NGPA K and H Value Computer Program (14) and Coefficients for the 1957 NGPSA Engineering Data Book K Charts (14).

The former provided equilibrium stage flash calculations using the Chao-Seader correlation. For this case, product distributions for the

individual stages were estimated. Then the liquid and vapor entering a given stage were combined to provide the feed stream for the flash model. The K values for each component were expressed as a power series in temperature for the absorber program.

Differences between these values and those obtained by the primary method reflected two things. First, they differed as to the feed to an equilibrium stage from estimated to actually calculated values. Second, they included the errors introduced when fitting the K values to the equation used in the absorber program. The equation used in this version of the program was

$$\ell n\ K = A + B/T + C/T^2$$

where A, B, and C were the regression coefficients and T, the Rankine temperature divided by one hundred.

Another readily available source of equilibrium values employed was a computer program--Coefficients for the 1957 NGPSA Engineering Data Book K Charts. This program provided coefficients for the above equation directly from the convergence pressure K value data found in the 1957 NGPSA Engineering Data Book (5). Both of these secondary sources of equilibrium values have been available through the NGPA and have been frequently employed commercially.

Figures 15, 16, and 17 present equilibrium constants from these sources for methane, ethane, and propane. For all components the Coefficients for the 1957 NGPSA Engineering Data Book K Charts Program predicted values substantially lower than the Chao-Seader methods. Methane K-values were from 10 to 16 per cent below values from the Chao-Seader correlation. Ethane values were 25 per cent lower; and, propane

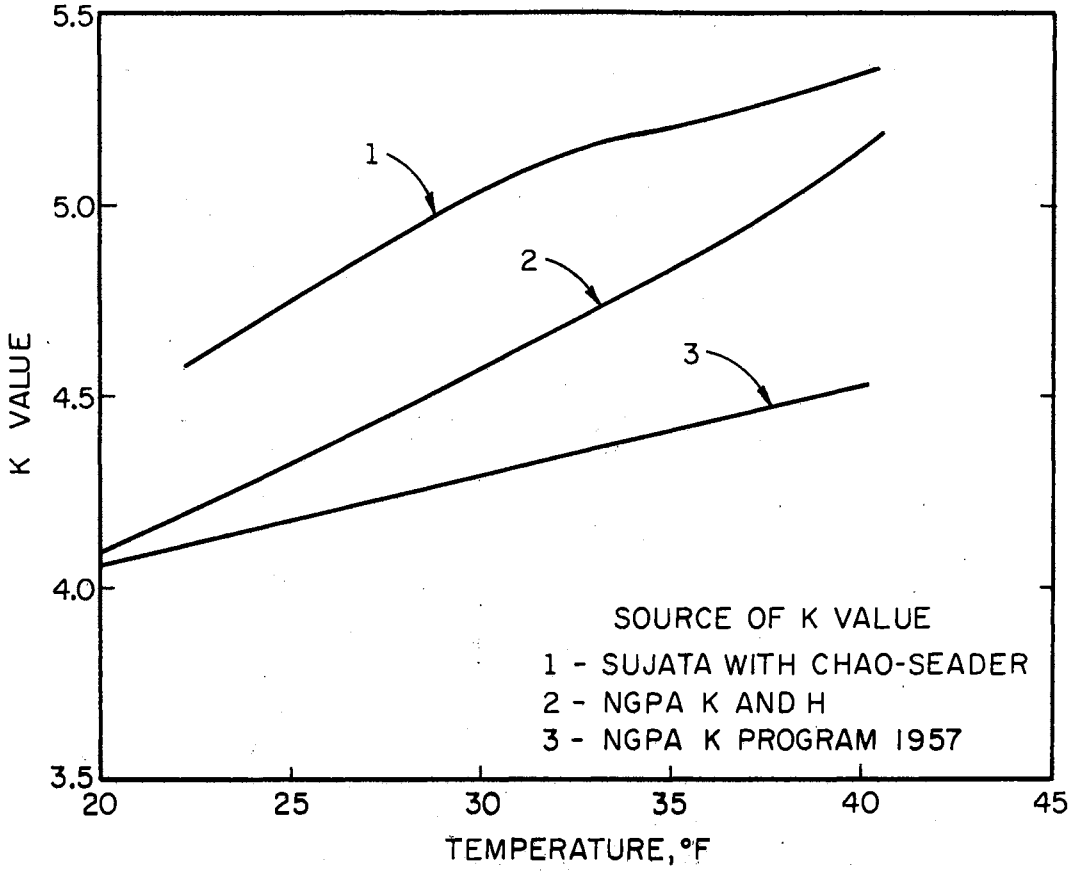

Figure 15. Source Dependence of Methane Equilibrium Values for A24 Test Period

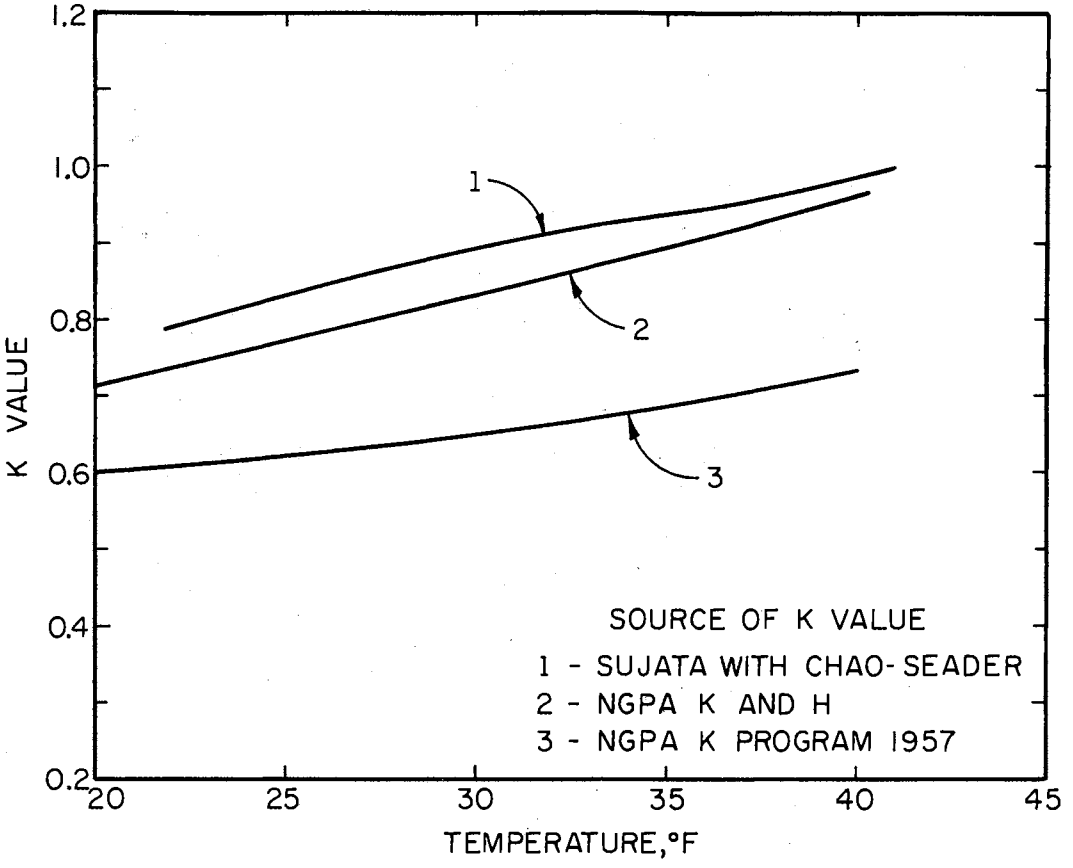

Figure 16. Source Dependence of Ethane Equilibrium Values for A24 Test Period

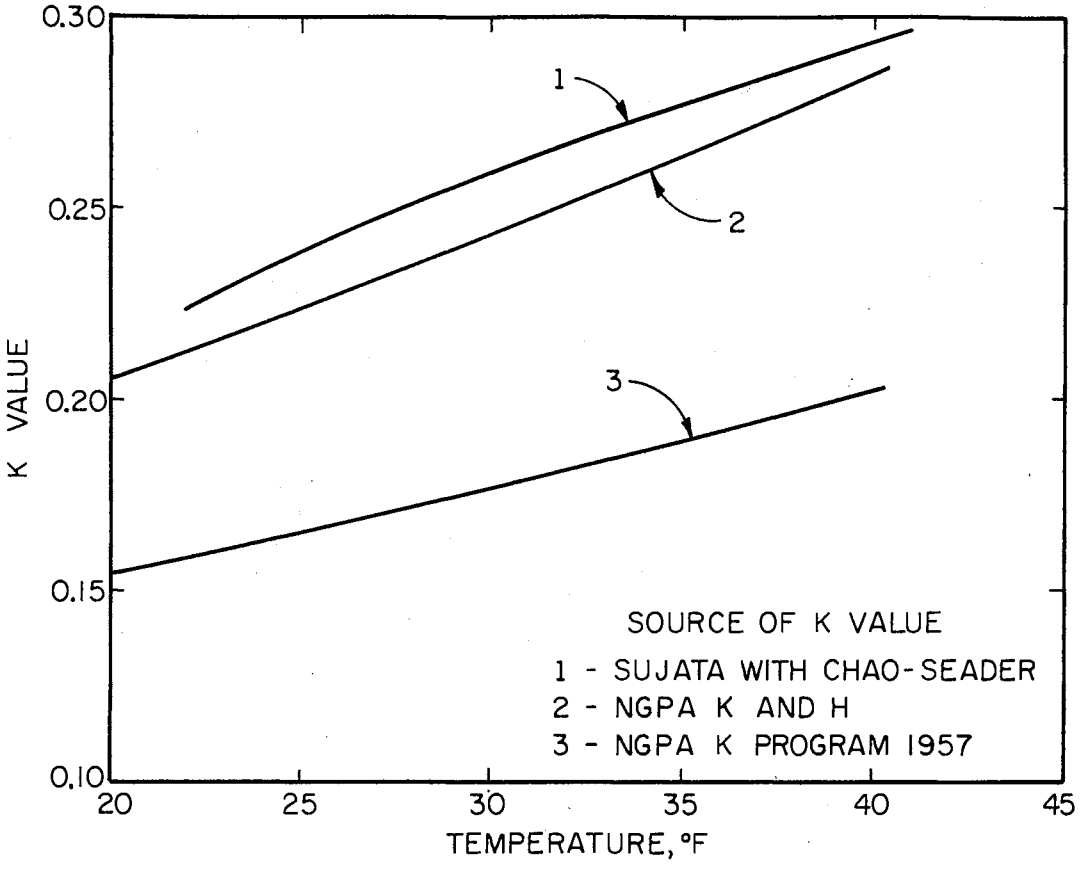

Figure 17. Source Dependence of Propane Equilibrium Values for A24 Test Period

was 30 per cent lower. The values from the off line Chao-Seader program, the NGPA K and H Value Computer Program, were also lower than those predicted by the hybrid program by about 3 to 8 per cent.

Results from absorber calculations employing K values from these sources are shown in Table XXV. Operating data from the A24 test period was used and eight theoretical trays were specified. As expected, results from calculations made with the smaller equilibrium values reported more complete absorption of the light hydrocarbons. In both cases employing the secondary sources, the overall absorption exceeded the experimental value while direct application of the Chao-Seader correlation did not reach the experimental value.

TABLE XXV

RESULTS FOR AN 8 TRAY MODEL OF THE A24 ABSORBER WITH DIFFERENT SOURCES

Variable	Experimental	Source		1957 K - Value Program
		Direct Chao-Seader	Indirect Chao-Seader	
Dry Gas				
Temperature, °F	45	40.7	44.3	45.5
Rate, moles/hr	92.323	92.545	91.826	91.884
C_1, mole per cent	86.150	85.896	86.144	86.348
C_2, mole per cent	6.417	6.423	6.287	6.249
C_3, mole per cent	1.553	1.751	1.594	1.430
Rich Oil				
Temperature, °F	22	22	20.7	26.6

Comparison of the experimental results with those obtained from stagewise calculations did not lead to exact matches in component recoveries or product conditions. Using the combined stagewise calculations and thermodynamic properties program one could not predict the light hydrocarbon recoveries found in the actual test runs regardless of the number of theoretical trays employed. The uncertainty introduced by the experimental data produced greater changes in the calculated solutions than could be made by increasing the number of stages.

Apparently, research grade data could not be obtained from industrial equipment without additional instrumentation. However, even with more sophisticated equipment, the problem would not be resolved. For example, the studies made at various pressures produced changes in component recoveries that were less than those introduced by changing the characterization of the heavy oil fraction. Also, the source of the vapor-liquid equilibrium constants had a greater effect on the component recoveries than did the oil characterization, pressure, or number of theoretical stages. So not only more instrumentation but also a larger number of longer test periods and more experimental data on the thermodynamics of the system would be required to accurately model plant-scale natural gas absorbers. Unfortunately such things find their home in research laboratories rather than in the field.

Error Analysis

In evaluating experimental data, the affects of uncertainties in the measured quantities were investigated with regards to their influence on the absorber description. For this purpose a model was developed based upon the physical configuration employed at the Ambrose

Gasoline Plant. The material balance model required a measured lean oil rate, LO, and a measured dry gas rate, DG, plus complete component analyses of the rich and lean oil streams. For these analyses $\bar{X}_{RO}$ and $\bar{X}_{LO}$ represented the mole fraction summation of the heavy oil portion in the rich oil and lean oil samples. These quantities were used to calculate the two rates that could not be directly measured, the rich gas and rich oil rates.

For these simple absorbers, the material balance was completed as below.

$$LO = \text{measured}$$

$$DG = \text{measured}$$

$$RO = \left(\frac{\bar{X}_{LO}}{\bar{X}_{RO}}\right)LO$$

$$RG = (DG + RO) - LO$$

The individual flow rates were a function of the following independent variables.

$$LO = f(LO)$$

$$DG = f(DG)$$

$$RO = f(LO, \bar{X}_{LO}, \bar{X}_{RO})$$

$$RG = f(LO, RO, DG)$$

The total derivatives for these rates were taken.

$$dLO = dLO$$

$$dDG = dDG$$

$$dRO = \left(\frac{\partial RO}{\partial LO}\right)_{\bar{X}_{LO},\bar{X}_{RO}} dLO + \left(\frac{\partial RO}{\partial \bar{X}_{LO}}\right)_{LO,\bar{X}_{RO}} d\bar{X}_{LO} + \left(\frac{\partial RO}{\partial \bar{X}_{RO}}\right)_{LO,\bar{X}_{LO}}$$

$$dRG = \left(\frac{\partial RG}{\partial DG}\right)_{RO,LO} dDG + \left(\frac{\partial RG}{\partial RO}\right)_{DG,LO} dRO + \left(\frac{\partial RG}{\partial LO}\right)_{DG,RO} dLO$$

Evaluating the derivatives and substituting, the equations became functions of the measured quantities.

$$dLO = dLO$$

$$dDG = dDG$$

$$dRO = RO \left(\frac{dLO}{LO} + \frac{d\bar{X}_{LO}}{\bar{X}_{LO}} - \frac{d\bar{X}_{RO}}{\bar{X}_{RO}} \right)$$

$$dRG = dDG + RO \left(\frac{d\bar{X}_{LO}}{\bar{X}_{LO}} - \frac{d\bar{X}_{RO}}{\bar{X}_{RO}} \right) + \left(\frac{RO}{LO} - 1 \right) dLO$$

These equations were used to reflect the variation of the measured variables, DG, LO, $\bar{X}_{LO}$, and $\bar{X}_{RO}$ upon the dependent variables RO and RG.

For example, suppose the uncertainty in the measured lean oil rate was 1.0 per cent of its rate. In applying these equations to calculate the uncertainties in other rates, the following results were obtained.

$$dLO = 0.01\ LO$$

$$dDG = 0$$

$$dRO = 0.01\ RO$$

$$dRG = 0.01(RO - LO) .$$

The uncertainty in the calculated rich oil rate would be one per cent of the rich oil rate. The uncertainty in the rich gas rate would be one per cent of the difference in the rich oil and lean oil rate or one per cent of the total absorption. These equations were used

when the uncertainties in experimental values had been established.

Once the model had been developed for expressing the uncertainty of measured quantities in the material balance equations, the model was extended to predict the uncertainties of the calculated product compositions and rates. As a starting point for this portion of the model, the rigorous absorber equation was used as defined in equation 5.

$$v_1 = v_{n+1}\left(\frac{1}{\Sigma_A + 1}\right) + \ell_o\left(1 - \frac{1}{\Sigma_A + 1}\right) \tag{5}$$

Assuming none of the light hydrocarbons were present in the lean oil, the second term of the equation was dropped. The resulting equation was rearranged to give the ratio of product to feed for each of the light components. This was the fraction not absorbed which was denoted as δ.

$$\delta = \frac{v_1}{v_{n+1}} = \left(\frac{1}{\Sigma_A + 1}\right) \tag{17}$$

Assuming that some constant absorption factor could represent the entire tower, then the right hand portion of this equation was replaced by its mathematical equivalence.

$$\delta = \frac{v_1}{v_{n+1}} = \frac{A - 1}{A^{n+1} - 1}$$

Experimental values for v_1 and v_{n+1} were used to calculate this constant absorption factor for the actual operating conditions.

Next, the constant absorption factor was assumed to be directly proportional to the total lean oil rate, LO, and inversely proportional to both the rich gas rate, RG, and the equilibrium constant evaluated

at the average column conditions. The proportionality constant, μ, required for this equality was assumed to be constant for small changes in the system.

$$A = \mu \frac{LO}{RGxK}$$

The total differentials of δ and A were developed as shown.

$$\delta = f(A, n)$$

$$d\delta = \left(\frac{\partial \delta}{\partial A}\right)_n dA + \left(\frac{\partial \delta}{\partial n}\right)_A dn$$

$$A = f(LO, RG, K)$$

$$dA = \left(\frac{\partial A}{\partial LO}\right)_{RG,K} dLO + \left(\frac{\partial A}{\partial RG}\right)_{LO,K} dRG + \left(\frac{\partial A}{\partial K}\right)_{LO,RG} dK$$

Taking the appropriate derivatives and substituting the constant absorption factor yielded an equation for predicting changes in the absorption of the light hydrocarbons.

$$d\delta = \left[\frac{1}{A^{n+1} - 1} - \frac{(n+1)A^n}{A^{n+1} - 1}\right] dA + \left[\frac{-\delta A^{n+1} \ell nA}{A^{n+1} - 1}\right] dn \qquad (19)$$

For convenience, this change was expressed as the change in the dry gas rate for each component.

$$v_1 = \delta v_{n+1}$$

$$\frac{dv_1}{v_1} = \frac{d\delta}{\delta} + \frac{dv_{n+1}}{v_{n+1}}$$

The left hand term of this equation was the fraction change in recovery of the individual component. Finally, combination of these

equations produced the following equation to estimate the change in dry gas rate for individual light hydrocarbons.

$$\frac{dv_1}{v_1} = C_1 \frac{dLO}{LO} + C_2 \frac{dK}{K} + C_3 \frac{dRG}{RG} + C_4\, dn \qquad (20)$$

where

$$C_1 = \left[\frac{1}{A^{n+1} - 1} - \frac{(n+1)A^n \delta}{A^{n+1} - 1} \right] \frac{A}{\delta}$$

$$C_2 = -C_1$$

$$C_3 = 1 + C_2$$

$$C_4 = \frac{A^{n+1} \ln A}{A^{n+1} - 1}$$

The coefficients of variation were functions of two experimentally determined quantities--δ and A--and one parameter, the number of theoretical stages. Numerical values for these coefficients are presented in Table XXVI for methane, ethane, and propane. The experimental data from the A24 test period were used with three levels of the parameter n-8, 16 and 24 theoretical trays.

The coefficients from this table were employed in the following manner. Suppose the absorber during the A24 test period was operated such that it had eight theoretical stages. Then for methane, a one per cent increase in the lean oil produced a 0.03 per cent decrease in the methane in the dry gas. For ethane and propane, the same one per cent increase in the lean oil rate would have given a 0.21 and 1.14 per cent decrease in their respective dry gas rates. Thus, the recoveries for these components would have increased by those amounts.

A one per cent decrease in the equilibrium constants for those components would have produced the same results as the increase in lean oil rate. This was indicated by their respective coefficients of variation.

TABLE XXVI

VARIATION COEFFICIENTS FOR A24 ABSORBERS

	Component	δ	A	LO	RG	K	n
8	Methane	0.9687	0.0313	-0.0323	1.0323	0.0323	-1E-13
Trays	Ethane	0.8273	0.1727	-0.2088	1.2088	0.2088	-2E- 7
	Propane	0.46029	0.5416	-1.1450	2.1450	1.1450	-2E- 3
16	Methane	0.9687	0.0313	-0.0323	1.0323	0.0323	-9E-26
Trays	Ethane	0.8273	0.1727	-0.2088	1.2088	0.2088	-2E-13
	Propane	0.46029	0.5397	-0.1720	2.1720	1.1720	-2E- 5
24	Methane	0.9687	0.0313	-0.0323	1.0323	0.0323	-9E-38
Trays	Ethane	0.8273	0.1727	-0.2088	1.2088	0.2088	-2E-19
	Propane	0.46029	0.5397	-1.1730	2.1730	1.1730	-1E- 7

For the same case, a one per cent decrease in the rich gas rate would have decreased the dry gas rates for those components by 1.03, 1.21, and 2.14 per cent respectively.

From this model, an additional theoretical stage would have decreased the methane dry gas rate by 1×10^{-11} per cent. For ethane and propane, the addition would have decreased the component dry gas rates by 2×10^{-5} and 0.2 per cent.

In evaluation overall uncertainties in monitoring the actual absorber operating conditions, the errors in measured quantities must be obtained. Since insufficient data were available to statistically estimate these variations, they were empirically estimated. These values were taken only as order of magnitude approximations.

- Dry Gas Rate--±5 per cent. The volume flow rate was determined from an orifice meter.
- Lean Oil Rate--±10 per cent. The volume flow rate was again obtained from an orifice meter. However, the conversion from volumetric to molar rates introduced more uncertainty.
- Component Analyses--±2 per cent of the component concentration.
- Equilibrium Constants--±10 per cent. This value accommodated uncertainty in K-values themselves and the uncertainties in the temperature and pressure measurements.

The uncertainties in the measured rates expressed as factors in the general equations are shown in the following equations.

$$\text{Lean Oil:} \quad \frac{dLO}{LO} = \pm 0.10$$

$$\text{Dry Gas:} \quad \frac{dDG}{DG} = \pm 0.05$$

The uncertainties for the rich oil and rich gas streams were calculated by applying equations 15 and 16.

$$\text{Rich Oil:} \quad \frac{dRO}{RO} = \pm\left(\frac{dLO}{LO} + \frac{d\bar{X}_{LO}}{\bar{X}_{LO}} + \frac{d\bar{X}_{RO}}{\bar{X}_{RO}} \right) = \pm 0.14$$

$$\text{Rich Gas:} \quad \frac{dRG}{RG} = \pm \left\{ 0.05\frac{DG}{RG} + \left(\frac{d\bar{X}_{LO}}{\bar{X}_{LO}} + \frac{d\bar{X}_{RO}}{\bar{X}_{RO}} \right) \frac{RO}{RG} + 0.1\frac{(RO-LO)}{RG} \right\} = \pm 0.059$$

These values were based upon measured quantities obtained from the A24 test period. Applying equation 20 with the variation coefficients from Table XXVI, the maximum uncertainty in the predicted dry gas concentration was calculated from the following equations.

$$\text{Methane:} \quad \frac{dv_1}{v_1} = -0.0323 \frac{dLO}{LO} + 1.0323 \frac{dRG}{RG} + 0.0323 \frac{dK}{K}$$

$$\text{Ethane:} \quad \frac{dv_1}{v_1} = -0.2088 \frac{dLO}{LO} + 1.2088 \frac{dRG}{RG} + 0.2088 \frac{dK}{K}$$

$$\text{Propane:} \quad \frac{dv_1}{v_1} = -1.1450 \frac{dLO}{LO} + 2.1450 \frac{dRG}{RG} + 1.1450 \frac{dK}{K}$$

The maximum uncertainties for an eight tray model are presented in Table XXVII. The effect of adding or subtracting one tray was approximated from the coefficient of variation. For all three components the uncertainty exceeded the effect of one tray change. For propane the uncertainty was more than twice the change produced by an additional stage. This lack of resolution was critical in the evaluation of this absorber test data.

Comparison of Parallel Operated Absorber

Up to this point all discussion has been directed toward the individual absorber test periods. The following tables have been presented to take advantage of the unique configuration of the parallel absorbers operating at nearly the same conditions but with a different number of actual trays. The major advantage of this configuration was that only the individual dry gas compositions were required for the comparison since the rich gas and lean oil streams were split to feed the individual towers. Other advantages were: the feed stream compositions and

temperatures were identical; the lean oil rates did not require precise conversion to molar rates; and measurements for the two absorbers were required only to be relative to each other.

TABLE XXVII

UNCERTAINTIES IN MEASURED VARIABLES MANIFESTED IN THE COMPONENT DRY GAS RATES FOR THE A24 TEST PERIOD

	Methane	Ethane	Propane
Per Cent	6.9	11.3	35.5
Moles*	5.48	0.67	0.50
Change Produced by Additional Stage, moles	1×10^{-11}	2×10^{-5}	0.1

*Basis: 100 moles/hr Rich Gas.

The four tests at the Ambrose Gasoline Plant were made in two sets. The first set included a simple 24 tray absorber operated in parallel to an eight tray tower. Both the rich gas and lean oil streams were common to the two units. In the second set, a 16 tray tower was run in parallel with the 24 tray column. The results from the two sets have been summarized in Table IX.

In the first period, a 24 tray absorber was operated in parallel to an eight tray absorber. The pressure of the 24 tray, A24, absorber was nine psi higher than that of the eight tray absorber, A8. The dry gases from both absorbers were combined immediately after being metered

individually and were nearly the same pressure. Since the pressures reported were measured at the rich oil port, the pressure difference was roughly the difference in pressure drop across the trays plus experimental error in the measurement.

The rich gas rates were specified equal since the basis for all calculations was 100 moles of rich gas per hour. The lean oil rates differed less than 0.8 per cent. Physically, this was not the case as more oil and gas were fed to the A8 absorber--the lower pressure absorber. However, with the change of basis, the lean oil rates became almost identical.

The A8 absorber recovered more gas, 8.015 moles, the A24, 7.677 moles. This was 4.4 per cent increase over the A24 value. This additional recovery was reflected in the methane, ethane, and propane recoveries. Here component recoveries are the moles removed from the rich gas divided by the moles of rich gas for each component.

$$\text{Recovery} = \frac{V_{n+1}-V_1}{V_{n+1}}$$

The increase in recovery for each component compared to the A24 absorber has been shown in Table XXVIII.

For each of the light hydrocarbons, the recovery was greater for the absorber with 8 trays than the absorber with 24 trays. However, this difference in recoveries was less than that introduced by the experimental errors in measurements. With only two, or even four test periods, insufficient data were available for specific statistical conclusions.

Results for the second set of test periods, Table XXIX, were generally the same as for the first set. For either set, however, very

little difference was observed in the recovery of the light hydrocarbons regardless of the number of actual trays employed.

TABLE XXVIII

COMPARISON OF LIGHT HYDROCARBON RECOVERIES FOR PARALLEL ABSORBERS OPERATED WITH 24 AND 8 TRAYS

Component	Recovery		Recovery with 8 trays / Recovery with 24 trays
	A24	A8	
Methane	0.0307	0.0326	1.062
Ethane	0.1752	0.1967	1.123
Propane	0.5917	0.6413	1.084

TABLE XXIX

COMPARISON OF LIGHT HYDROCARBON RECOVERIES FOR PARALLEL ABSORBERS OPERATED WITH 24 AND 16 TRAYS

Component	Recovery		Recovery with 16 trays / Recovery with 24 trays
	A24	A8	
Methane	0.0593	0.0448	0.755
Ethane	0.2269	0.2354	1.037
Propane	0.6317	0.6567	1.040

CHAPTER VII

CONCLUSIONS AND RECOMMENDATIONS

The following conclusions and recommendations are offered for the results of absorber tests made at the Cities Service Oil Company, Ambrose Gasoline Plant in Blackwell, Oklahoma.

Evaluation of Experimental Data

1. Flow rates. The lean oil and dry gas streams were adequately measured although calibrated orifice coefficients would have improved the accuracy of those measurements. Since the rich oil and rich gas rates could not be measured, the burden of completing the material balance fell on the two measured streams.

2. Temperatures. All measured temperatures could be obtained with reasonable accuracy with the thermometers available. Two changes are recommended to provide improved monitoring of the absorber operation. First, the individual dry gas temperature should be measured. This would provide a complete heat balance around the unit. Second, if possible the stream temperatures should be measured as close as possible to the entrance and exit ports.

3. Samples. The sample analysis provided by Cities Service Oil Company and Phillips Petroleum Company appear to be excellent. The sampling technique could be improved with minor modification to the operating units. For example the rich gas sample should have been

taken immediately prior to entering the absorber. Also the rich oil stream should be sampled from the exit stream rather than the sight glass.

4. Material Balance Calculations. Closing the overall material balance for the individual absorbers did not appear to be a problem when the heavy fraction balance was employed. However, the rich oil composition calculated from the individual material balances differed substantially from the analytical results for the light hydrocarbons. Again, by having to use the heavy oil fraction to calculate the rich oil and then rich gas rates, no extra information was available to resolve this difference.

5. Flash Calculations-- Vapor-liquid equilibrium calculation on the feed and product streams were made using the Chao-Seader correlation to predict the thermodynamic properties. Results for the lean oil, rich gas, and dry gas streams gave the proper phase for the streams. For the rich oil stream, all results predicted a two phase mixture from 2 to 18 per cent vapor. These results along with component material balance calculations indicated a rich oil sample that contained too much light hydrocarbons. Duplicate sample analyses repeated the original results and further reinforced the conclusion that the rich oil sampling procedure may not have been an accurate sample of the stream leaving the unit.

6. Heat Balance Calculations. With the individual dry gas temperatures unavailable and the uncertainty of the calculated rich oil and rich gas rates, the heat balanace calculations could only indicate possible problems. These deviations were larger than could be

attributed to heat leaks into the absorbers. The uncertainty in each case appeared to be in evaluating the rich oil conditions.

Comparison With Tray-by-Tray Solutions

1. Direct Comparison. In each of the four absorber tests, direct comparison of the experimental results with those of the tray-by-tray solutions showed that the light hydrocarbon recoveries of the plant scale units exceeded results provided by the model. Even when the number of ideal trays equalled the number of actual stages, the predicted recoveries were below experimental values. These differences prompted the investigation of three variables that indirectly affected the calculated component recoveries.

2. Pressure. Calculated results obtained at ten psia above and below the measured pressure indicated more recovery at the highest pressure. The increased recoveries were not sufficient to match experimental values. The changes produced by the variations in operating pressure revealed that any correction for pressure drop per stage would be minor when compared to the existing differences between experimental and calculated recoveries.

3. Oil Characterization. The carbon number distribution for the heavy fraction of the oil stream represented the progress made in analysis brought by the gas chromatograph. Parallel to this development was that of the vapor-liquid equilibrium correlations such as the Chao-Seader correlation used in this work. The calculated absorber solutions obtained with different characterizations of the oil fraction illustrated the importance of this variable. Solutions obtained for different characterizations varied more than did solutions obtained

with 24 and 4 trays. The proper characterization of the oil fraction as it affects the light hydrocarbon vapor-liquid equilibrium values should be well defined before attempting to model experimental absorber data.

4. Source of Vapor-Liquid Equilibrium Data. The source of vapor-liquid equilibrium constants like the oil characterization had a larger effect on the predicted light hydrocarbon recoveries than the number of theoretical stages. Both of the studies indicated the need for more complete vapor-liquid equilibrium data for the system being studied. Whether this information be obtained from more complete characterization of the heavy components, from improved correlations, or from experimental data, it should be obtained before any further studies are made for the effectiveness of natural gas absorbers.

Comparison of Parallel Test Runs

In the comparison of the experimental data with tray-by-tray calculations, some problems were encountered in selecting the equilibrium constants. These problems tended to overshadow the determination of the number of ideal stages required to produce similar recoveries of the light hydrocarbons. In obtaining the experimental data from parallel absorbers this problem did not interfer with the comparison of these results.

Results from the two sets of test periods show only small differences in the recoveries for first 24 and 8 trays and then 26 and 16 trays. For the comparison, the dry gas compositions were used directly to give the light hydrocarbon recoveries. In both sets of test runs, the tower with fewer trays appeared to give as good as or better recoveries.

These deviations were small and were thought to be the result of small differences in column operating conditions.

The use of parallel absorbers appears to offer the best method for determining the effectiveness of plant scale natural gas absorbers. Evidence from this work indicated that little or no loss of production would occur. Such future work would require modification of the test absorber and installation of flow meters for the rich gas and rich oil streams for both units. By operating the parallel absorbers for some reasonable period at identical conditions and taking several samples of each stream, the relative effectiveness of the contact stage could be determined without research level vapor-liquid equilibrium data as required for comparison with rigorous modelling.

SELECTED BIBLIOGRAPHY

1. Brown, G. G., and M. Souders, Jr. Ind. Eng. Chem., 24 (1932), 519.

2. Chao, K. C. and J. D. Seader, A. I. Ch. E. Journal, 7, 4 (June, 1961), 598.

3. Edmister, W. C., The Petroleum Engineer, 18, 13 (September, 1947).

4. Edmister, W. C., A. I. Ch. E. Journal, 3, 2 (June, 1957), 165.

5. Engineering Data Book. Natural Gas Processors Suppliers Association, Seventh Edition, Tulsa, Oklahoma (1957).

6. Engineering Data Book. Natural Gas Processors Suppliers Association, Eighth Edition, Tulsa, Oklahoma (1966).

7. Erbar, J. H., Private communication.

8. Erbar, J. H., C. L. Persyn, W. C. Demister, Proceedings of the 43rd Annual Convention, Natural Gas Processors Association March 11-13, 1964, New Orleans, Louisiana.

9. Holland, C. D., Multicomponent Distillation, Prentice-Hall, Inc., 1963.

10. Hull, R. J., and K. Raymond, Oil & Gas J., (Nov. 9, 16, 23, and 30, December 7, 14, and 28, 1953).

11. Lewis, W. K., and G. L. Matheson, Ind. Eng. Chem., 24 (May, 1932), 494.

12. "The Analysis of Natural Gases," Natural Gas Processors Association Bulletin 2261-6A, Tulsa, Oklahoma.

13. "Coefficients for the 1957 NGSMA Engineering Data Book K Charts," Natural Gas Processors Association, Tulsa, Oklahoma.

14. "The NGPA K & H Value Computer Program," Natural Gas Processors Association, Tulsa, Oklahoma.

15. Nelson, W. L., Petroleum Refinery Engineering, McGraw-Hill Book Company, Inc., 1958.

16. Owens, W. R., "Short-Cut Absorber Calculations With Incorporated Heat Balances," M. S. Thesis, Oklahoma State University, Stillwater, Oklahoma (1968).

17. Owens, W. R., and R. N. Maddox, Ind. Eng. Chem., 60, 12 (December, 1968).

18. Rackett, H. G., Private communication.

19. Ravicz, A. E., "Non-Ideal Stage Multicomponent Absorber Calculations by Automatic Digital Computer," Ph.D. Thesis, University of Michigan, Ann Arbor, Michigan (1959).

20. Smith, B. D., Design of Equilibrium Stage Process, McGraw-Hill Book Company, Inc. (1963).

21. Spear, R. R., "An Evaluation of the Sujata Absorption Calculation Method," M. S. Thesis, Oklahoma State University, Stillwater, Oklahoma (1966).

22. Sujata, A. D., Petrol. Refiner., 40, 12 (December, 1962), 137.

23. Thiele, E. W., and R. L. Geddes, Ind. Eng. Chem., 25 (March, 1933), 289.

24. Wilson, G. M., and S. T. Barton, "K-Values in Highly Aromatic and Highly Napthenic Real Oil Absorber Systems." Research Report-2, Natural Gas Processors Association (March 1971).

NOMENCLATURE

Upper Case

A	Absorption factor defined as A = L/KV
C	Number of components
G	Heat balance error for individual stage
H	Total stream enthalpy
K	Component equilibrium constant
L	Total liquid rate leaving a tray, moles
Q	Net error in overall heat balance
S	Stripping factor defined as S = KV/L
T	Temperature, ^{o}R
V	Total vapor rate leaving a tray, moles
$\bar{X}_j$	Summation of liquid mole fractions for j and heavier components

Lower Case

f_i	Moles of particular component entering as feed on tray i
i	Index for the tray
j	Index for the component
l_i	Component j liquid rate leaving tray i, moles
n	Total number of trays; also refers to bottom tray
n+1	Refers to rich gas stream
t_i	Temperature on stage i
v	Component j vapor rate leaving tray i, moles

0 Refers to lean oil stream

1 Refers to top tray

Miscellaneous

α_j Ratio of $\bar{X}_j$ to $\bar{X}_{C8}$

δ Fraction of j not absorbed

μ Proportionality constant for equation 18

Π_A $A_1A_2A_3 \ldots A_n$

Σ_A $A_1A_2A_3 \ldots A_n + A_2A_3 \ldots A_n + \ldots + A_n$

DG Dry gas stream

LO Lean oil stream

RG Rich gas stream

RO Rich oil steam

APPENDIX A

STREAM ANALYSIS

The lean oil and rich oil analyses were made by the Phillips Petroleum Company at their Bartlesville Research Laboratory. Their procedure was as follows.

The rich oils were repressurized to approximately 1000 psig with ethylene glycol. The hydrocarbon phase was sampled and split by distillation between components containing five carbon atoms and those containing six. The lighter components were determined from procedures outlined in NGPA Bulletin 2261-6A, "The Analysis of Natural Gases" (12).

The C_6 and heavier materials for both rich and lean oils were analyzed on two gas-liquid chromatograph capillary columns. The C_6 and lighter components were individually identified on a 150 foot by 0.01" ID squalane capillary. A 150' x 0.01" ID DC-550 column was used to determine the distribution of carbon numbers in the C_7 and heavier portions.

ASTM sulfonation procedures on the morning lean oil sample indicated approximately 10% aromatics in the C_7 plus fraction. This value was used as a typical value in correcting the DC-550 column's tendency to elute aromatic compounds with components with one more carbon on the chain.

The complete oil analyses are shown in Tables XXX and XXXI. The complete list included 27 components, of which several were present in

TABLE XXX

COMPLETE OIL ANALYSES FOR A24 AND A8 TEST PERIODS

Component	Rich Oil		Lean Oil
	24 Tray Absorber	8 Tray Absorber	
	Mole Per Cent	Mole Per Cent	Mole Per Cent
Nitrogen	0.52	0.55	--
Methane	19.4	22.9	0.01
Ethane	9.5	9.8	0.04
Carbon Dioxide	0.10	0.12	--
Propane	15.1	14.2	0.03
Isobutane	2.55	2.14	0.01
n-Butane	5.6	4.6	0.10
Isopentane	1.04	0.80	0.25
n-Pentane	1.08	0.85	0.43
Cyclopentane	0.02	0.03	0.06
Neohexane	<0.01	0.01	0.01
2,3-Dimethylbutane	0.04	0.03	0.03
2-Methylpentane	0.18	0.16	0.24
3-Methylpentane	0.10	0.10	0.16
n-Hexane	0.31	0.29	0.58
Methylcyclopentane 2,2-Dimethylpentane	0.15	0.17	0.31
Benzene	0.02	0.03	0.03
Cyclohexane	0.21	0.32	0.53
Heptanes	2.17	2.08	4.9
Octanes	4.8	4.5	10.5
Nonanes	4.7	4.6	10.5
Decanes	7.5	7.3	16.7
Undecanes	12.2	12.0	26.9
Dodecanes	9.5	9.4	20.9
Tridecanes	3.1	2.88	6.5
Tetradecanes+	0.10	0.20	0.32
	99.99	99.97	100.02

TABLE XXXI

COMPLETE OIL ANALYSES FOR B24 AND B16 TEST PERIODS

Component	Rich Oil		Lean Oil
	24 Tray Absorber	8 Tray Absorber	
	Mole Per Cent	Mole Per Cent	Mole Per Cent
Nitrogen	0.45	--	--
Methane	25.6	31.7	0.01
Ethane	10.9	10.9	0.04
Carbon Dioxide	0.16	0.16	--
Propane	16.00	13.3	0.03
Isobutane	2.73	1.99	0.01
n-Butane	6.5	4.1	0.07
Isopentane	1.38	0.48	0.22
n-Pentane	1.57	0.54	0.43
Cyclopentane	<0.01	0.02	0.03
Neohexane	<0.01	0.01	0.01
2,3-Dimethylbutane	0.18	0.01	0.03
2-Methylpentane	0.39	0.13	0.24
3-Methylpentane	0.17	0.07	0.15
n-Hexane	0.25	0.21	0.56
Methylcyclopentane 2,2-Dimethylpentane	0.08	0.11	0.30
Benzene	<0.01	0.01	0.03
Cyclohexane	0.01	0.15	0.46
Heptanes	1.20	1.62	4.5
Octanes	3.2	3.8	10.3
Nonanes	3.6	3.9	10.4
Decanes	5.8	6.2	16.7
Undecanes	9.5	10.1	27.1
Dodecanes	7.4	7.8	21.2
Tridecanes	2.53	2.48	6.6
Tetradecanes+	0.42	0.23	0.60
	100.01	100.02	100.0

in only small amounts. To facilitate calculations, two groupings were used to reduce the number of components required for the characterization of the oil to 20 components and then to 12 components. The 20 component characterization resulted from combining the trace components with components with the same number of carbon atoms. The 12 component characterization was produced by grouping components not in the rich gas stream into three fractions--C_{6+}, C_{8+}, and a heavy component C_{15+}. Table XXXII presents these groupings.

The gas analysis was by components except for a fraction labeled C_{6+}. In this study this fraction was treated as a 50-50 mixture of hexane and heptane.

TABLE XXXII

COMPONENT GROUPING FOR 20 COMPONENT AND 12 COMPONENT OIL CHARACTERIZATION

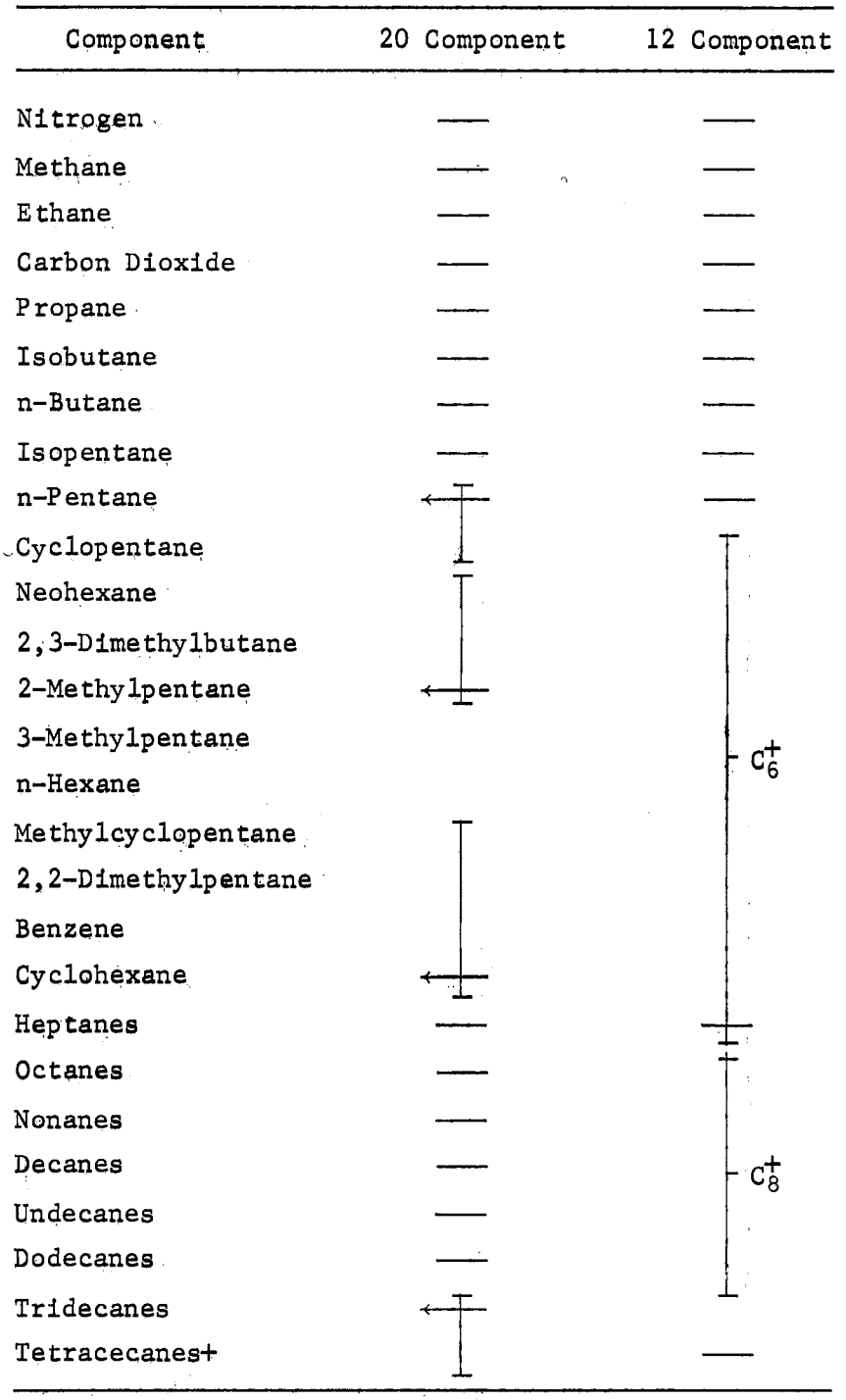

APPENDIX B

COMPUTER PROGRAMS

Several computer programs have been used in this work. The fundamentals of these programs are presented in this appendix. The programs fell into two basic categories--tray-by-tray absorber programs and thermodynamic data source programs.

Absorber Programs

Two major programs used to solve absorber problems were tray-by-tray programs. Both used the Sujata technique for reaching a solution, but differed in the manner in which thermodynamic properties were obtained. The program authored by Spear (21) used equilibrium and enthalpy values obtained from polynomial expressions in temperature for each component. The modified form of the program evaluated the thermodynamic properties as they were required using the Chao-Seader correlation.

The basic program used about 1/5 of the computer time required for the Sujata-Chao-Seader ensemble with identical initial temperatures and convergence limits. The heat balance convergence limit was expressed as a fraction of the total feed enthalpy. In the basic program with a reasonable initial temperature profile, convergence was generally reached with this limit at 0.05 per cent. With improved initial tray temperatures the limit could be reduced to 0.01 per cent.

For the modified program, solution was usually achieved with 0.5 per cent heat balance error limit. When temperatures could be estimated within 1.0°F, the limit could be reduced to about 0.1 per cent.

The limiting feature for both programs was the convergence to heat balance. The temperature convergence subroutine for both programs had a maximum number of iterations specified. If the correct heat balance was not found within that number of tries the calculations were aborted. The same limitations were applied to the material balance procedures; however, limits of 0.01 per cent of the total feed were used for both programs with no problems.

Thermodynamic Data Source Programs

The NGPA K and H Value Computer Program (14) was used to generate equilibrium and enthalpy values for each component. Preliminary calculations gave composition profiles for the A24 absorber. The liquid and vapor entering each tray were combined for the feed to the flash equilibrium program. The temperature and pressure were specified; pressure measured and temperature taken from preliminary calculations. These liquid and vapor enthalpies and equilibrium constants obtained from this program were fitted to appropriate polynomials in temperature by a least-squares procedure. These constants are reported in Appendix C.

The NGPA Equilibrium Constant Program (13) was used to provide a secondary source of equilibrium values. These values were obtained from a regression model of the G. G. Brown Charts in the 1957 NGPSA Engineering Data Book (5). Program output included not only equilibrium values but also the polynomial coefficients that were used by the absorber program.

The secondary source of enthalpy values was the Kellogg Charts in the NGPSA Engineering Data Book (5). Pure component total heats were tabulated for the required components. An author written program developed the required coefficients for the temperature range and pressure requested.

Program Synopsis

Absorber Program--Sujata

Program input-problem identification, column variables, control variables component names, convergence limits, feed conditions and molar rates, thermodynamic properties coefficients, temperature limits, and initial temperature profile were included.

- All thermodynamic properties are functions of temperature only expressed as $^{o}R/100$.
- Material balance convergence limit was 0.01 per cent total feed.
- Heat balance convergence limit varied from 0.1 to 0.01 per cent total feed enthalpy depending upon the quality of the initial temperature profile.

Absorber Program--Sujata With Chao-Seader

Program input included problem identification, column and control variables, component identification code, convergence limits, feed conditions and molar rates, and initial temperature profile.

- Material balance convergence limit was 0.01 per cent of total feed.
- Heat balance error limit varied from 0.5 to 0.05 per cent of total feed enthalpy. With reasonable initial temperature profile a limit of 0.1 per cent could be used.

- Hypothetical components may be used according to Chao-Seader correlation programmed by Erbar (8).

Thermodynamic Data Source Program--

NGPA K and H Value Computer Program

Program input included problem identification, number of components, temperature, pressure and component identification key and molar rates.

- Option specified to flash the feed at specified temperature and pressure to find the correct liquid product to feed ratio--option 5.
- A print out of partial enthalpies of the liquid and vapor was required.

Thermodynamic Data Source Program--

NGPA K Program

Program input included problem identification, temperature range required, temperature spacing between equilibrium values required for fitting data to polynomial, pressure of the system, temperature scale factor, and the component identity code.

- A convergence pressure at 5000 psia is used. The calculated convergence pressure for the A24 rich oil was 4500 psia. The Hadden method (5) was used to calculate the system convergence pressure. In the 500 psia system, this change in convergence pressure had little effect on the K-values.
- Temperature range for the data was $-20^{\circ}F$ to $80^{\circ}F$.
- Delta T, the spacing, was chosen as $10^{\circ}F$.
- Coefficients required temperature to be expressed in $^{\circ}R/100$.

Thermodynamic Data Source Program--

Kellogg Enthalpies

Program input included problem identification, number of components, pressure, molecular weight of component if not paraffinic, temperature scale, and component identification.

- Temperature range for liquid enthalpy was -60°F to 220°F; for vapor 0° - 220°F.
- Output had units of Btu/lb mole.
- Coefficients required temperature to be expressed in °R/100.

APPENDIX C

THERMODYNAMIC PROPERTIES

While the majority of the calculations made for this work employed equilibrium and enthalpy values from an incorporated Chao-Seader correlation, several runs were made with thermodynamic data from other sources. This was done for two reasons. First the effect of secondary sources for thermodynamic data was investigated. Second, the computer time required for calculations was reduced using the polynomial equations to predict the thermodynamic properties.

Polynomial coefficients for other data are presented in Tables XXXIII through XXXVII for these equations.

$$\ell n K_i = A + B/T + C/T^2$$

$$H_i^V = A + BT + CT^2$$

$$H_i^\ell = A + BT + CT^2$$

where

$$T = {}^\circ R/100$$

Table XXXIII presents the Coefficients from the NGASA Engineering Data Book K Charts (13) obtained with 5000 psi convergence pressure. The enthalpy data were obtained from the Kellogg Charts of the 1957 NGPSA Engineering Data Book (5). These data were obtained for an operating pressure of 545 psi.

TABLE XXXIII

EQUILIBRIUM AND ENTHALPY COEFFICIENTS AT 545 PSIA FROM 1957 NGPSA ENGINEERING BOOK

Component	A	B	C	D
	Equilibrium Constant Coefficients at 545.000 Psia			
Carbon Dioxide	0.15432262E 01	0.83120413E 01	-0.75312500E 02	
Nitrogen	0.22197968E 02	-0.15566330E 03	0.29618750E 03	
Methane	0.27814837E 01	-0.36663637E 01	0.26659842E 01	-0.74005112E 02
Ethane	0.14984407E 01	0.20602302E 02	-0.27874951E 03	0.52819482E 03
Propane	0.44620998E-01	0.48313354E 02	-0.43458667E 03	0.77650171E 03
i-Butane	0.43407196E 00	0.39636337E 02	-0.40291870E 03	0.67831543E 03
n-Butane	0.27361596E 00	0.46381866E 02	-0.47390723E 03	0.84300439E 03
i-Pentane	0.16193419E 01	0.20815842E 02	-0.34577490E 03	0.56564697E 03
n-Pentane	0.37043095E 00	-0.16829987E 02	-0.13701279E 03	0.16816739E 03
2-Methylpentane	-0.77164268E 00	0.44330750E 01	-0.11468750E 03	
3-Methylpentane	-0.18100061E 01	0.10283750E 02	-0.12162500E 03	
n-Hexane	-0.60312204E 04	0.46146210E 02	-0.20118750E 03	
Cyclohexane	-0.19381226E 02	0.14974480E 03	-0.39407007E 03	
n-Heptane	-0.11754589E 02	0.89023666E 02	-0.29850000E 03	
n-Octane	-0.17218979E 02	0.12965479E 03	-0.39300000E 03	
n-Nonane	-0.26460968E 02	0.20685210E 03	-0.57331250E 03	
n-Decane	-0.26437088E 02	0.19470079E 03	-0.53656250E 03	
n-Undecane	-0.31550476E 02	0.23202379E 03	-0.61733569E 03	
n-Dodecane	-0.34421249E 02	0.24828079E 03	-0.64840625E 03	
n-Tridecane	-0.45489746E 02	0.34417188E 03	-0.87233179E 03	
	Vapor Phase Enthalpy Coefficients			
Carbon Dioxide	0.70968848E 03	0.73937085E 03	0.18046860E 02	
Nitrogen	0.70968848E 03	0.73937085E 03	0.18046860E 02	

TABLE XXXIII (CONTINUED)

Component	A	B	C	D
Methane	0.70968848E 03	0.73937085E 03	0.18046860E 02	
Ethane	0.78539429E 03	0.13793870E 04	0.21343750E 02	
Propane	0.54155742E 04	0.39844141E 03	0.15125000E 03	
i-Butane	0.78226992E 04	0.11260829E 03	0.21785699E 03	
n-Butane	0.78226992E 04	0.11260829E 03	0.21785699E 03	
i-Pentane	0.90492148E 04	0.25657690E 03	0.24656250E 03	
n-Pentane	0.90492148E 04	0.25657690E 03	0.24656250E 03	
2-Methylpentane	0.90492148E 04	0.25657690E 03	0.24656250E 03	
3-Methylpentane	0.90492148E 04	0.25657690E 03	0.24656250E 03	
n-Hexane	0.98145000E 04	0.48938062E 03	0.26912500E 03	
Cyclohexane	0.98145000E 04	0.48938062E 03	0.26912500E 03	
n-Heptane	0.10549438E 05	0.60715405E 03	0.30806250E 03	
n-Octane	0.11671777E 05	0.74385229E 03	0.34662500E 03	
n-Nonane	0.13203316E 05	0.71550366E 03	0.39975000E 03	
n-Decane	0.14193047E 05	0.86279272E 03	0.43737500E 03	
n-Undecane	0.15526688E 05	0.86833960E 03	0.48750000E 03	
n-Dodecane	0.16694367E 05	0.91403491E 03	0.54300000E 03	
n-Tridecane	0.17667848E 05	0.10140618E 04	0.57606250E 03	
	Liquid Phase Enthalpy Coefficients			
Carbon Dioxide	0.81078882E 03	-0.81500366E 03	0.25710913E 03	
Nitrogen	0.81078882E 03	-0.81500366E 03	0.25710913E 03	
Methane	0.81078882E 03	-0.81500366E 03	0.25710913E 03	
Ethane	-0.17583118E 04	0.97042221E 02	0.23512889E 03	
Propane	-0.81532397E 03	-0.26030249E 03	0.30505054E 03	
i-Butane	-0.30441169E 04	0.58933398E 03	0.27937085E 03	
i-Pentane	-0.50670742E 04	0.13091790E 04	0.26318750E 03	
n-Pentane	-0.50670742E 04	0.13091790E 04	0.26318750E 03	

TABLE XXXIII (CONTINUED)

Component	A	B	C	D
2-Methylpentane	-0.50670742E 04	0.13091790E 04	0.26318750E 03	
3-Methylpentane	-0.50670742E 04	0.13091790E 04	0.26318750E 03	
n-Hexane	-0.71570938E 04	0.20105010E 04	0.26062500E 03	
Cyclohexane	-0.71570938E 04	0.20105010E 04	0.26062500E 03	
n-Heptane	-0.95949922E 04	0.28511169E 04	0.24125000E 03	
n-Octane	-0.87760781E 04	0.23287830E 04	0.35243750E 03	
n-Nonane	-0.88792070E 04	0.21731748E 04	0.43293750E 03	
n-Decane	-0.99901250E 04	0.24166208E 04	0.47375000E 03	
n-Undecane	-0.11118469E 05	0.26573079E 04	0.52681250E 03	
n-Dodecane	-0.12241828E 05	0.28871670E 04	0.57475000E 03	
n-Tridecane	-0.13409629E 05	0.31230779E 04	0.62262500E 03	

TABLE XXXIV

EQUILIBRIUM AND ENTHALPY COEFFICIENTS AT 545 PSIA
FROM NGPA K AND H PROGRAM

Component	A	B	C
Equilibrium Constant Coefficents at 545 Psia			
Carbon Dioxide	1.54323	8.31204	-75.31250
Nitrogen	22.19797	-155.66320	296.18750
Methane	12.76430	-82.44122	134.12500
Ethane	11.38357	-77.57205	102.31250
Propane	8.31856	-56.02744	40.93750
i-Butane	5.06378	-34.08420	-9.81250
n-Butane	5.68551	-41.25253	1.93750
i-Pentane	-0.18046	3.27188	-96.06250
n-Pentane	-0.41469	5.13309	-106.81250
2-Methylpentane	-0.77164	4.43307	-114.68750
3-Methylpentane	-1.81001	10.28375	-121.62500
n-Hexane	-6.03122	46.14621	-201.18750
Cyclohexane	-19.38124	149.74470	-394.07030
n-Heptane	-11.75459	89.02368	-298.50000
n-Octane	-17.21899	129.65480	-393.00000
n-Nonane	-26.46098	206.85200	-573.31250
n-Decane	-26.43710	194.70080	-536.56250
n-Undecane	-31.55048	232.02380	-617.33590
n-Dodecane	-34.42126	248.28080	-648.40620
n-Tridecane	-45.48975	344.17210	-872.33200
Vapor Phase Enthalpy Coefficients			
Carbon Dioxide	-3649.66200	1361.46700	-4.93750
Nitrogen	72.26929	763.86740	-18.43750
Methane	1614.76100	-118.13130	107.37500
Ethane	-5149.60100	1752.42500	6.75000
Propane	-10741.39000	3374.57500	-72.93750
i-Butane	-12495.78000	3506.64200	1.37500
n-Butane	-6619.83200	1195.32300	251.43750
i-Pentane	-16899.46000	4836.02300	-42.00000
n-Pentane	-11507.98000	2734.46800	184.00000
2-Methylpentane	-13417.82000	2899.72200	241.00000
3-Methylpentane	-12049.78000	2643.13300	274.00000
n-Hexane	-9354.90200	1444.91700	403.00000
Cyclohexane	-14195.51000	2724.23800	181.00000
n-Heptane	-13810.21000	2815.95200	340.00000
n-Octane	-17955.82000	4149.54600	300.00000
n-Nonane	-14639.28000	2379.25300	569.00000
n-Decane	-19113.64000	3833.00300	505.00000
n-Undecane	-27066.62000	6751.12500	288.00000
n-Dodecane	-27859.98000	6713.21800	376.00000
n-Tridecane	-20129.21000	3253.97700	810.00000

TABLE XXIV (CONTINUED)

Component	A	B	C
	Liquid Phase Enthalpy Coefficients		
Carbon Dioxide	12315.17000	-6355.15200	705.00000
Nitrogen	-39200.53000	15010.96000	-1270.93700
Methane	-19962.42000	6925.32400	-504.06250
Ethane	-20298.67000	5811.80000	-350.06250
Propane	-15993.44000	3052.46400	-16.12500
i-Butane	-10430.71000	302.41350	298.87500
n-Butane	-10800.00000	453.17230	283.12500
i-Pentane	-1893.69500	-3463.75300	698.06250
n-Pentane	-1882.26100	-3475.71000	699.31250
2-Methylpentane	-1012.15600	-4446.86700	834.43750
3-Methylpentane	3147.51600	-5745.84300	957.25000
n-Hexane	8503.16700	-7891.52700	1155.62500
Cyclohexane	30648.71000	-16819.83000	1891.62500
n-Heptane	17094.53000	-11564.64000	1535.06200
n-Octane	24935.17000	-14888.82000	1897.62500
n-Nonane	32574.89000	-18092.01000	2240.62500
n-Decane	38730.69000	-20656.69000	2520.50000
n-Undecane	47711.80000	-24314.87000	2911.75000
n-Dodecane	55569.37000	-27550.35000	3263.37500
n-Tridecane	62533.62000	-30371.17000	3570.00000

TABLE XXXV

EQUILIBRIUM AND ENTHALPY COEFFICIENTS AT 536 PSIA
FROM NGPA K AND H PROGRAM

Component	A	B	C
Equilibrium Constant Coefficients			
Carbon Dioxide	1.62641	7.79437	-74.45313
Nitrogen	22.56322	-159.12420	304.81250
Methane	13.34654	-87.92767	147.37500
Ethane	11.46259	-78.07428	103.12500
Propane	8.23173	-54.87085	37.50000
i-Butane	5.00941	-33.17999	-12.87500
n-Butane	5.04556	-34.66104	-14.93750
i-Pentane	0.18759	0.14703	-89.62500
n-Pentane	1.31402	-11.19489	-68.37500
2-Methylpentane	0.74327	-9.78735	-81.50000
3-Methylpentane	-2.05311	13.15097	-129.93750
n-Hexane	-5.14776	38.10382	-183.12500
Cyclohexane	-19.55168	151.97990	-401.07810
n-Heptane	-10.18932	74.44696	-264.87500
n-Octane	-17.78899	135.86430	-410.00000
n-Nonane	-20.86227	153.24980	-445.50000
n-Decane	-28.15588	212.16610	-581.25000
n-Undecane	-34.08734	257.55150	-681.93350
n-Dodecane	-32.82851	233.78390	-616.14840
n-Tridecane	-42.48865	316.05490	-807.21480
Vapor Phase Enthalpy Coefficients			
Carbon Dioxide	-4048.82700	1543.76300	-24.93750
Nitrogen	-409.13960	957.97650	-38.00000
Methane	-5330.54600	2746.7 800	-187.62500
Ethane	-3705.62400	1182.28500	63.68750
Propane	-8783.90600	2608.24800	3.06250
i-Butane	-15801.03000	4919.15200	-147.62500
n-Butane	-7764.45700	1721.39200	193.37500
i-Pentane	-10204.55000	2145.58500	230.00000
n-Pentane	-4755.00700	22.60156	458.00000
2-Methylpentane	-1148.28400	-2073.98800	747.00000
3-Methylpentane	-9074.62800	1498.07000	386.00000
n-Hexane	-12390.82000	2777.14100	260.00000
Cyclohexane	-13629.44000	2576.36600	190.00000
n-Heptane	-491.13280	-2575.78100	888.00000
n-Octane	-17821.64000	4200.83900	287.00000
n-Nonane	-15914.78000	3023.86600	494.00000
n-Decane	-21686.16000	5023.36300	373.00000
n-Undecane	-19000.80000	3570.52000	605.00000

TABLE XXXV (CONTINUED)

Component	A	B	C
n-Dodecane	-14895.62000	1524.35400	899.00000
n-Tridecane	-7935.95300	-1609.58200	1299.00000
Liquid Phase Enthalpy Coefficients			
Carbon Dioxide	12450.12000	-6413.77700	711.12500
Nitrogen	-42374.67000	16321.46000	-1405.93700
Methane	-20042.89000	6958.82400	-507.56250
Ethane	-20541.30000	5914.22600	-361.06250
Propane	-17357.80000	3615.09400	-74.18750
i-Butane	-9587.65600	-46.15112	334.81250
n-Butane	-10660.91000	394.54390	289.25000
i-Pentane	-2168.30900	-3353.89100	687.06250
n-Pentane	-1769.44800	-3525.47200	704.75000
2-Methylpentane	-1482.97900	-4256.94500	815.31250
3-Methylpentane	2735.10400	-5580.44100	940.68750
n-Hexane	8223.68300	-7781.78100	1144.87500
Cyclohexane	35918.26000	-18998.67000	2116.62500
n-Heptane	17115.69000	-11580.53000	1537.43700
n-Octane	23746.42000	-14407.98000	1849.06200
n-Nonane	32054.03000	-17888.05000	2220.75000
n-Decane	40365.14000	-21342.89000	2592.37500
n-Undecane	47773.05000	-24354.42000	2917.31200
n-Dodecane	55531.55000	-27550.51000	3265.06200
n-Tridecane	61645.69000	-30022.80000	3536.00000

TABLE XXXVI

EQUILIBRIUM AND ENTHALPY COEFFICIENTS AT 575 PSIA

Component	A	B	C
Equilibrium Constant Coefficients			
Carbon Dioxide	1.27778	9.94461	-77.95313
Nitrogen	22.52422	-159.13430	303.93750
Methane	12.80459	-83.39304	136.68750
Ethane	10.99244	-74.65387	96.62500
Propane	7.98691	-53.85135	37.81250
i-Butane	5.62307	-40.77435	9.37500
n-Butane	3.69053	-23.15323	-38.93750
i-Pentane	-2.17766	21.16949	-135.62500
n-Pentane	0.45183	-4.78058	-78.87500
2-Methylpentane	-1.78421	12.59863	-130.00000
3-Methylpentane	-3.52721	25.26263	-153.37500
n-Hexane	-7.30368	56.74982	-222.12500
Cyclohexane	-21.73416	170.68220	-439.58980
n-Heptane	-9.65004	66.60376	-238.50000
n-Octane	-19.17342	146.40490	-427.18750
n-Nonane	-22.93044	170.09730	-476.87500
n-Decane	-27.65067	203.75320	-550.39840
n-Undecane	-35.01631	262.73190	-682.97650
n-Dodecane	-36.76442	267.86300	-686.32420
n-Tridecane	-44.66998	332.82390	-834.52730
Vapor Phase Enthalpy Coefficients			
Carbon Dioxide	-3748.32700	1340.38300	1.56250
Nitrogen	452.03660	622.23510	-5.31250
Methane	-2620.58100	1610.39500	-69.62500
Ethane	-7239.82800	2529.32200	-67.25000
Propane	-5431.30800	1050.58000	176.06250
i-Butane	-2944.27700	-605.63670	437.43750
n-Butane	-14714.25000	4340.92100	-58.56250
i-Pentane	-14341.30000	3551.51100	107.00000
n-Pentane	-9822.03100	1803.69000	297.00000
2-Methylpentane	-16839.85000	4036.06200	144.00000
3-Methylpentane	-17062.57000	4432.36700	110.00000
n-Hexane	-17344.00000	4453.50700	114.00000
Cyclohexane	-18267.21000	4108.73400	60.00000
n-Heptane	-13411.14000	2327.05400	414.00000
n-Octane	-18632.17000	4060.81200	336.00000
n-Nonane	-16918.28000	2911.12300	544.00000
n-Decane	-17071.14000	2546.05400	670.00000
n-Undecane	-27129.07000	6295.50700	370.00000
n-Dodecane	-23918.94000	4572.78900	634.00000

TABLE XXXVI (CONTINUED)

Component	A	B	C
n-Tridecane	-18881.33000	2193.46500	959.00000
Liquid Phase Enthalpy Coefficients			
Carbon Dioxide	12256.08000	-6320.92500	701.18750
Nitrogen	-36092.64000	13721.87000	-1137.93700
Methane	-19682.19000	6808.67500	-491.87500
Ethane	-20410.48000	5849.98000	-352.50000
Propane	-16287.96000	3171.80100	-27.87500
i-Butane	-9605.71400	-33.47168	333.25000
n-Butane	-9390.77300	-123.00340	342.12500
i-Pentane	-1191.38600	-3742.48300	725.75000
n-Pentane	-850.35540	-3890.15200	740.93750
2-Methylpentane	-873.32810	-4491.08200	837.62500
3-Methylpentane	4139.87100	-6139.72200	996.25000
n-Hexane	9205.71800	-8163.96000	1181.93700
Cyclohexane	34788.33000	-18497.35000	2061.62500
n-Heptane	18303.94000	-12040.05000	1581.62500
n-Octane	27057.30000	-15734.58000	1931.68700
n-Nonane	34153.82000	-18708.55000	2300.50000
n-Decane	41650.96000	-21820.60000	2636.12500
n-Undecane	49350.87000	-24945.83000	2971.93700
n-Dodecane	57069.94000	-28118.87000	3316.56200
n-Tridecane	64245.69000	-31021.28000	3631.00000

TABLE XXXVII

EQUILIBRIUM AND ENTHALPY COEFFICIENTS AT 565 PSIA

Component	A	B	C
Equilibrium Constant Coefficients			
Carbon Dioxide	1.36350	9.42365	-77.12891
Nitrogen	21.88361	-152.81170	288.81250
Methane	12.30245	-78.33011	124.31250
Ethane	11.00807	-74.51297	95.81250
Propane	7.88908	-52.55331	33.93750
i-Butane	4.25701	-27.09055	-24.81250
n-Butane	6.63767	-51.34653	28.43750
i-Pentane	-0.49527	5.33228	-98.50000
n-Pentane	1.12435	-10.80844	-65.56250
2-Methylpentane	-1.13487	6.84976	-117.56250
3-Methylpentane	-1.77319	8.79013	-114.93750
n-Hexane	-4.94044	34.37827	-169.43750
Cyclohexane	-19.74629	152.00450	-396.01560
n-Heptane	-12.51899	95.12320	-309.56250
n-Octane	-18.85197	143.99830	-423.43750
n-Nonane	-26.99443	210.36340	-576.93750
n-Decane	-29.41298	221.77650	-596.83590
n-Undecane	-29.34120	208.62390	-554.71480
n-Dodecane	-35.75681	259.13520	-668.35150
n-Tridecane	-41.57387	303.87570	-767.69920
Vapor Phase Enthalpy Coefficients			
Carbon Dioxide	-4140.30000	1522.79500	-18.68750
Nitrogen	90.58398	766.09130	-19.62500
Methane	-454.28440	723.34520	21.37500
Ethane	-4386.23800	1382.40000	48.75000
Propane	-8637.80800	2417.51800	32.06250
i-Butane	-9470.74600	2142.12900	150.37500
n-Butane	-8079.65200	1671.91700	211.43750
i-Pentane	-942.40230	-1888.51100	661.00000
n-Pentane	-10220.01000	2047.85200	266.00000
2-Methylpentane	-7136.39000	131.69920	539.00000
3-Methylpentane	-21373.94000	6300.62100	-89.00000
n-Hexane	-16852.78000	4346.64800	118.00000
Cyclohexane	-16368.62000	3425.69800	123.00000
n-Heptane	-7721.27300	92.35938	636.00000
n-Octane	-20594.17000	4992.87100	231.00000
n-Nonane	-14413.07000	2016.50800	626.00000
n-Decane	-28094.23000	7238.18700	176.00000
n-Undecane	-21245.91000	4033.52700	591.00000
n-Dodecane	-25872.76000	5554.28100	520.00000

TABLE XXXVII (CONTINUED)

Component	A	B	C
n-Tridecane	-21629.07000	3509.97700	810.00000
Liquid Phase Enthalpy Coefficients			
Carbon Dioxide	12006.25000	-6221.14400	691.00000
Nitrogen	-35116.67000	13322.57000	-1096.93700
Methane	-20863.01000	7295.32000	-542.00000
Ethane	-20304.35000	5808.80000	-348.75000
Propane	-16559.37000	3284.26200	-39.62500
i-Butane	-9138.55400	-227.20610	353.25000
n-Butane	-9996.25700	125.05540	316.68750
i-Pentane	-1058.71000	-3800.62100	732.06250
n-Pentane	-708.96090	-3951.87100	747.62500
2-Methylpentane	-548.01170	-4629.39400	852.31250
3-Methylpentane	2677.35800	-5542.11700	935.25000
n-Hexane	8966.36700	-8070.96400	1172.93700
Cyclohexane	33804.69000	-18100.76000	2021.62500
n-Heptane	17998.05000	-11921.44000	1570.18700
n-Octane	25583.10000	-15136.60000	1921.12500
n-Nonane	33694.76000	-18530.33000	2283.31200
n-Decane	40397.89000	-21317.23000	2585.68700
n-Undecane	49135.94000	-24871.82000	2965.87500
n-Dodecane	56382.69000	-27851.85000	3290.81200
n-Tridecane	64227.94000	-31031.80000	3634.00000

Tables XXXIII through XXXVII present coefficients obtained from a least squares fit of data from the NGPA K and H Value Computer Program for each test period. From the solution of the Sujata with Chao-Seader program of the A24 case, a representative composition profile was obtained. The feed streams entering a tray were combined and used as a single feed in the NGPA K and H Value Computer Program. This stream was flashed providing equilibrium and enthalpy values at the specified pressure. This was repeated for several trays producing thermodynamic data which was fitted solely as a function of temperature at the specified pressure. A latent dependence upon composition was inherent in these constants.

These coefficients were used with the basic program to generate initial temperature profiles for extended work with the combined program. They also provided the starting point for investigation of all variables.

APPENDIX D

CALCULATION OF STREAM RATES

Of the four streams crossing the boundaries of each absorber, only the lean oil and the dry gas rates were measured. They were measured by orifice meters and logged by separate flow recorders. The procedures used to convert the static and differential pressures to volumetric and molar rates have been presented below.

Lean Oil Volumetric Rate

The procedure followed that described in the NGPSA Engineering Data Book (5), page 10, using the equation

$$Q_h = C' \sqrt{h_w M}$$

where

Q_h = gallons per hour

C' = orifice constant ($F_b \times F_{gt} \times F_r$)

h_w = differential pressure of water

F_b = orifice factor

F_{gt} = specific gravity - temperature factor

F_r = Reynolds number factor

M = meter factor for direct reading charts.

Conditions at the meter:

diameter of orifice 4.25 inches
diameter of tube 6.065 inches

$F_b = 4216.6$

Flowing temperature = 33^oF
Estimated specific gravity @ 60^oF = 0.735

$F_{gt} = 1.1830$

Viscosity at 33^oF = 1.4 centipoise
= 30.85 Saybolt Seconds (15)
Average h_w = 36.24
Reynolds number = $dDh_w/spgr$ = 1270.9

$F_r = 1.001$

$C' = 4993.2$

M for chart range 0-100 = 1.00

$MC' = 4993.2$

Table XXXVIII shows the volumetric lean oil rates.

TABLE XXXVIII

VOLUMETRIC LEAN OIL RATES

Absorber	$\sqrt{h_w}$	gal./hr.	gal./min.
AM24	5.92	29560	493
AM8	6.11	30510	509
PM24	6.03	30110	502
PM16	6.02	30100	502

Dry Gas Volumetric Rate

The source of this procedure was identical with that of the lean oil. The equation has been presented below.

$$Q_h = C' \sqrt{h_w P_f}$$

where

Q_h = flow rate, base condition

C' = orifice flow constant

h_w = differential pressure, inches of water

P_f = static pressure absolute

$C' = F_b \times F_{pb} \times F_{tb} \times F_g \times F_{tf} \times F_r \times Y \times F_{pv}$

with

F_b = basic orifice flow factor

F_{pb} = pressure base of factor

F_{tb} = temperature base factor

F_g = specific gravity factor

F_{tf} = flowing temperature factor

F_r = Reynolds number factor

Y = expansion factor

F_{pv} = supercompressibility factor

Conditions at the meter:

diameter of orifice 9.5 inches
diameter of tube 13.0 inches

Assumed 0.500" walls in 14" pipe

Calculated F_b $F_b = 21516.4$

Assumed pressure base - 14.73 psia

$F_{pb} = 1.0$

Assumed temperature base = $60^{o}F$

$$F_{tb} = 1.0$$

Specific gravity average all four dry gas streams

$$F_{g} = 1.26572$$

Average dry gas temperature $46.1^{o}F$

$$F_{tf} = 1.0136$$

Reynolds number factor

$$F_{r} = 1.00022$$

Expansion factor

$$Y = 0.99712$$

Supercompressibility factor

F_{pv} = $\sqrt{1/Z}$ where Z was evaluated from reduced temperature and pressure correlations.

$$F_{pv} = 1.0437$$

So, C' = 2.8734.

Table XXXIX shows the volumetric dry gas rates.

TABLE XXXIX

VOLUMETRIC DRY GAS RATES

Absorber	$h_w P_f$	MM scf/hr.
AM24	233.5	6.708
AM8	240.2	6.903
PM24	243.6	6.998
PM16	249.2	7.160

Conversion to Molar Rates

Converting the volumetric gas rates to molar rates was straight forward using the reduced temperature and pressure of each mixture and the compressibility factor.

The molar volume of the lean oil streams was determined by three methods. The first method found the liquid density from page 165 of the 1966 NGPSA Engineering Data Book (6). The second source was the NGPA K and H Value Computer Program (14) liquid density subroutine. This procedure was a mathematical model of the correlation presented in the 1956 NGPSA Engineering Book (5). The final method of determining liquid volumes was by a correlation of critical compressibility and critical volumes as a function of reduced temperatures. This correlation, developed by H. G. Rackett (18), has been shown to predict accurate liquid densities for a wide range of systems.

Rackett's correlation has been used extensively for this work to predict the molar lean oil rate from the measured volumetric rate. For the A series of test periods the lean oil molar volume was 3.156 ft^3/mole. The molar volume for the B series was 3.160 ft^3/mole. Molar volumes from the other sources were about five per cent lower than these values predicted by Rackett's equation. This difference resulted in the larger estimated uncertainty in the measurement of the lean oil rate.

APPENDIX E

APPROXIMATE HEAT TRANSFER TO TEST ABSORBERS

The following calculations were made to give an order of magnitude value for the rate of heat transfer to the absorbers from the environment. The rate of heat transfer is the product of the heat transfer coefficient, U; the surface area of the absorber, A; and the driving force of the temperature difference, ΔT. The heat transfer coefficient was taken from a series of articles by R. J. Hull and K. Raymond (10). The value assumed was 3.0 Btu/ft^2°F hr. The area was that calculated for a 57 foot cylinder eight feet in diameter--1530 ft^2. The driving force was the difference between the ambient temperature, 60°, and the average tower temperature, 38°F--22°F. Using these values the heat gained by the absorber was

$$Q = U A \Delta T$$

$$Q = (3)(1530)(22)$$

$$Q = 1 \times 10^5 \text{ Btu/hr.}$$

The actual absorbers were operated at approximately 20,000 moles of rich gas per hour or 200 times the basis for tray-by-tray calculations. Using this scale factor the heat gained by an average absorber on the reduced basis, Q', was

$$Q' = \frac{1 \times 10^5 \text{ Btu/hr}}{200} = 500 \text{ Btu/hr}$$

This was the average heat transfer for all absorbers.

VITA

William Russ Owens

Candidate for the Degree of

Doctor of Philosophy

Thesis: AN EXPERIMENTAL STUDY OF THE EFFECTIVENESS OF PLANT SCALE NATURAL GAS ABSORBERS

Major Field: Chemical Engineering

Biographical:

Personal Data: Born in Memphis, Tennessee, June 28, 1944, the son of Francis M. and Lillian E. Owens.

Education: Attended grade school in Marianna, Arkansas; graduated Salutatorian of T. A. Futrall High School in Marianna in 1962; received Bachelor of Science Degree from the University of Arkansas in 1966; received the Master of Science degree from Oklahoma State University in May, 1968; completed requirements for the Doctor of Philosophy degree in May, 1973.

Membership in Scholarly or Professional Societies: Pi Mu Epsilon, Omega Chi Epsilon, American Institute of Chemical Engineers.

Professional Experience: Summer employment by Texaco in 1956; employed since June, 1970, as Chemical Engineer with Texaco's Port Arthur Research Laboratory in Port Arthur, Texas.